# HYDRODYNAMIC STUDY
# OF
# TAPERED FLUIDIZED BED

A THESIS SUBMITTED IN PARTIAL FULFILLMENT OF THE
REQUIREMENTS FOR THE DEGREE OF

**Master of Technology**

**in**

**Chemical Engineering**

By

**K.GOBORDHAN PATRO**


**Department of Chemical Engineering**
**National Institute of Technology**
**Rourkela**
**2007**

# HYDRODYNAMIC STUDY OF TAPERED FLUIDIZED BED

A THESIS SUBMITTED IN PARTIAL FULFILLMENT OF THE REQUIREMENTS FOR THE DEGREE OF

**Master of Technology**

**in**

**Chemical Engineering**


By

**K.GOBORDHAN PATRO**

Under the guidance of

**Prof. (Dr.) K.C.BISWAL**




**Department of Chemical Engineering**
**National Institute of Technology**
**Rourkela**


**2007**


**NATIONAL INSTITUTE OF TECHNOLOGY**
**ROURKELA**

# CERTIFICATE

This is to certify that the thesis entitled, "HYDRODYNAMIC STUDY OF TAPERED BED" submitted by Sri K.GOBORDHAN PATRO in partial fulfillment of the award of Master of Technology Degree in CHEMICAL Engineering with specialization in "Coal Chemical & Fertilizers" at the National Institute of Technology**,** Rourkela (Deemed University) is an authentic work carried out by him under my supervision and guidance. To the best of my knowledge, the matter embodied in the thesis has not been submitted to any other University/Institute for the award of any Degree or Diploma.

Date

**Prof. (Dr.) K.C.BISWAL**
Dept.of Chemical Engg.
**N**ational **I**nstitute of Technology
Rourkela-769008

# ACKNOWLEDGEMENT

I express my sincere gratitude to my guide, **Dr. K.C. Biswal,** Prof. of the Department of Chemical Engg. , National Institute of Technology, Rourkela for giving me this great opportunity to work under his kind support, guidance and constructive criticism in the completion of my project .

I offer my deepest appreciation for people who assisted me in the experiments, And I would like to thank to all those who are directly or indirectly supported me in carrying out this thesis work successfully.

K.Gobordhan Patro

# CONTENTS

**Page No**.

# ABSTRACT

Hydrodynamic characteristics of fluidization in conical or tapered beds differ from those in columnar beds due to the variation of superficial velocity in the axial direction of the beds. In the former, fixed and fluidized regions could coexist and the sharp peaking of the pressure drop could occur, thereby giving rise to a remarkable pressure drop-flow rate hysteresis loop at incipient fluidization. To explore these unique properties, a series of experiments was carried out in gas-solid tapered fluidized beds with various tapering angles. Detailed visual observations of fluid and Particle behavior and measurements of the pressure drops have led to the identification of five flow regimes. The tapering angle of the beds has been found to dramatically affect the beds' behavior. Other hydrodynamic characteristics determined experimentally included the maximum pressure drop, minimum velocity of partial fluidization and minimum velocity of full fluidization. Models have been proposed to quantify the hydrodynamic characteristics of gas-solid tapered fluidized beds. The results predicted by the models compare favorably with experimental data. Naturally, the models are applicable to gas-solid columnar fluidized beds corresponding to the tapered beds with a tapering angle of zero.

Fluidization operations in cylindrical columns are extensively used in process industries. But, in a number of these operations, the particles are generally not of uniform size or there may be reduction in size due to chemical reactions like combustion or gasification, or attrition. In cylindrical beds, the particle size reduction results in entrainment, limitation of operating velocity in addition to the other demerits like slugging, non-uniform fluidization generally associated with such beds. These disadvantages are overcome by use of tapered beds to conduct fluidization operation. This is due to conduct fluidization operation. This is due to the gradual reductions of superficial velocity of the fluid because of increase in cross sectional area with height. However, in general the particles are not of uniform size in the feed itself and also there may be particle size reduction during operation in fluidized beds. Hence,the study of hydrodynamic characteristics of such beds is essential in the operation of such beds.

Based on dimensional analysis, correlations have been developed with the system parameters viz., geometry of tapered bed, particle diameter, static bed height, density of solid and gas and superficial velocity of the fluidizing medium.

Correlations have been developed for some characteristics specially, critical fluidization velocities and maximum bed pressure drops of gas – solid tapered fluidized bed of binary mixture of regular particles. Experimental values of critical fluidization velocities and maximum bed pressure drops have been compared with the developed correlations.

# LIST OF FIGURES

**Page No.**

# LIST OF TABLES

**PageNo.**

# CHAPTER 1

## INTRODUCTION

# INTRODUCTION TO TAPERED BED

Fluidization is the operation by which fine solids are transformed into a fluid like state through contact with a gas or solid. This method of contacting has a number of unusual characteristics, and fluidization engineering is concerned with efforts to take advantage of this behavior & put it to good use.

The ease with which particles fluidize and the range of operating conditions which sustain fluidization vary greatly among gas-solid systems. Whether the solids are free flowing or not, whether they are liable to agglomerate, static charges, vessel geometry, gas inlet arrangement, and other factors affect the fluidization characteristics of a system.

Conical fluidized bed is very much useful for the fluidization of wide distribution of particles, since the cross sectional area is enlarged along the bed height from the bottom to the top, therefore the velocity of the fluidizing medium is relatively high at the bottom, ensuring fluidization of the large particles and relatively low at the top, preventing entrainment of the small particles.

Since the velocity of fluidizing medium at the bottom is fairly high, this gives rise to low particle concentration, thus resulting in low reaction rate and reduced rate of heat release. Therefore the generation of high temperature zone near the distributor can be prevented.

Due to the existence of a gas velocity gradient along the height of a conical bed, it has some favorable special hydrodynamic characteristics. The conical bed has been widely applied in many industrial processes such as

[1] Biological treatment of waste-water,
[2] Immobilized biofilm reaction,
[3] Incineration of waste-materials,
[4] Coating of nuclear fuel particles,
[5] Crystallization, roasting of sulfide ores,
[6] Coal gasification and liquefaction,
[7] Catalytic polymerization,
[8] Fluidized contactor for sawdust and mixtures of wood residues and
[9] Fluidization of cohesive powder.

The study of the hydrodynamic characteristics of fluidization of conical beds is focused on two fields:
(1) liquid–solid systems and
(2) gas–solid systems.

For liquid–solid systems, the hydrodynamic characteristics of fluidization of conical beds, i.e. the fixed bed, partially fluidized bed and fully fluidized bed regimes, have been described by Kwauk [6] according to his theory of bubble less fluidization. Peng and Fan [1] systematically discussed the conditions for the transition of the flow regimes: when the buoyancy force exerted on the entire particle bed by fluid flowing upward is less than the effective gravitational force of the particle bed, the particles in the bed remain static, and this is the fixed bed regime.

When the particle weight in the top layer of the conical bed is equal to or less than the drag force by fluid flowing upward, the fully fluidized bed regime occurs. Between these two cases, the flow regime is called a partially fluidized bed regime. However, it is not easy to predict the characteristics of fluidization for the partially fluidized bed regime theoretically [1]. All these studies are based on the idealized fluidization defined by Kwauk [6], i.e. according to the following assumptions:

- The radial distribution of the fluid at any cross-section of the conical bed is uniform;
- There is no back mixing for the fluid phase;
- The frictional force between wall and particles is neglected.

For gas–solid systems in conical spouted beds, Olazar et al. [2] observed five flow regimes: fixed bed, partially fluidized bed, spouted bed, transition regime from spouted bed to jet spouted bed and jet spouted bed. The hydrodynamic characteristics for these five regimes are presented by empirical correlations [3]. The difficulty in predicting the hydrodynamics of fluidization from the theory of Peng and Fan possibly lies in the fact that the inlet diameter for the conical spouted bed is less than that of the bed bottom. The same approach by Peng and Fan [1] has been adopted by Gelperin et al. [4] and Nishi [5] for the incipient fluidization of gas–solid conical beds. However, they did not involve the other characteristics of fluidization in gas–solid conical beds.

The characteristics of fluidization in three flow regimes, namely fixed bed, partially fluidized bed and fully fluidized bed, are investigated using a conical bed with three different cone angles and a Geldart-D powder. The purpose is to:

- Determination of the flow regimes for gas–solid conical fluidized beds;
- Discussion of the idealized conditions of Peng and Fan [1];
- Discussion of the application of the correlations and
- Discussion of the local characteristics of fluidization.

## VARIABLES AFFECTING THE QUALITY OF FLUIDIZATION

Some of the variables affecting the quality of fluidization are:

- **Fluid inlet**: It must be designed in such a way that the fluid entering the bed is well distributed.
- **Fluid flow rate**: It should be high enough to keep the solids in suspension but it should not be so high that the fluid channeling occurs.
- **Bed height**: With other variables remaining constant, the greater the bed height, the more difficult it is to obtain good fluidization.
- **Particle size**: It is easier to maintain fluidization quality with particles having a wide range than with particles of uniform size.
- **Gas, Liquid and solid densities**: The closer the relative densities of the gas, liquid and the solid, the easier are to maintain smooth fluidization.
- **Bed internals**: In commercial fluidizers internals are provided to perform the following functions.

- To prevent the growth of bubble sizes
- To prevent lateral movement of fluid and solids.
- To prevent slug formation
- To prevent elutriation of fine particles

## STRUCTURE OF TAPERED BED

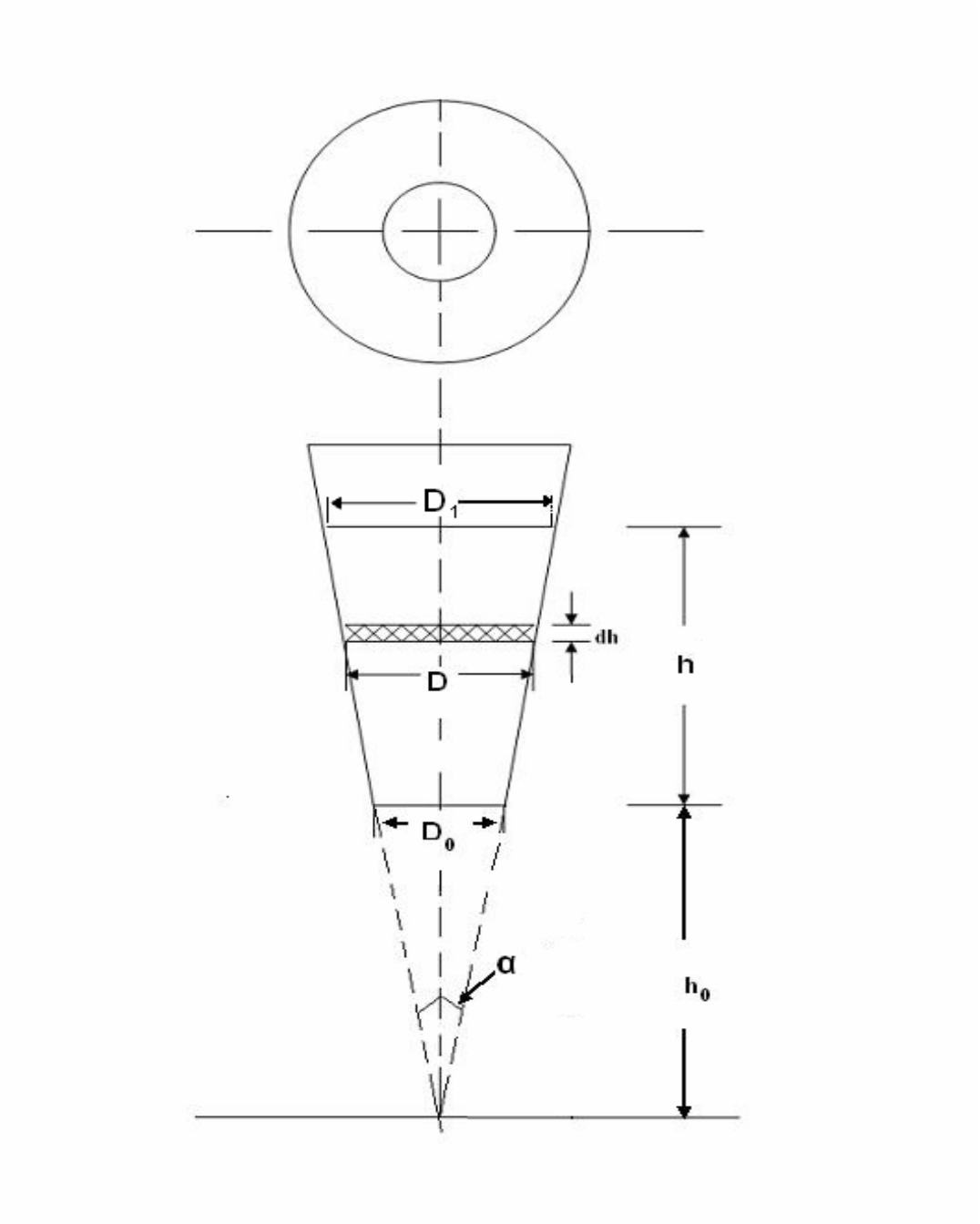


Fig-1.1

## THE PHENOMENON OF FLUIDIZATION:

On passing fluid (gas or solid) upward through a bed of fine particles, at a low flow rate fluid merely percolates through the void spaces between stationary particles. This is a fixed bed. With an increase in flow rate, particles move apart and a few are seen to vibrate and move about in restricted regions. This is the expanded bed.

At a still higher velocity, the pressure drop through the bed increases. At a certain velocity the pressure drop through the bed reaches the maximum and a point is reached when the particles are all just suspended in the upward flowing gas or liquid. At this moment, the particles at the bottom of the bed begin to fluidize, thereafter the condition of fluidization will extend from the bottom to the top and the pressure drop will decline fairly sharply.

Evidently, fluidization is initiated when the force exerted between a particle and fluidizing medium counterbalances the effective weight of the particle, the vertical component of the compressive force between the adjacent particles disappears, and the pressure drop through any section of the bed about equals the weight of fluid and particles in that section. The bed is considered to be just fluidized and referred to as an incipiently fluidized bed or a bed at minimum fluidization. Under the assumption that friction is negligible between the particles and the bed walls, also it is assumed that the lateral velocity of fluid is relatively small and can be neglected and the vertical velocity of the fluid is uniformly distributed on the cross sectional area.

Gas –solid systems generally behave in quite different manner. With an increase in flow rate beyond minimum fluidization, large instabilities with bubbling and channeling of gas are observed. At higher flow rates agitation becomes more violent and the movement of solids becomes vigorous. In addition, the bed does not expand much beyond its volume at minimum fluidization. Such a bed is called an aggregative fluidized bed, a heterogeneous fluidized bed, a bubbling fluidized bed, or simply a gas fluidized bed.

## EXPERIMENTAL PHENOMENA

### Flow regimes

A typical diagram of the hydrodynamic characteristics of the conical bed is shown in Fig.1.2 with the increase of superficial gas velocity, Ug0, the total pressure drop, ΔPt, varies along the line of O→A→B→C.
In the different stages, the hydrodynamic characteristics of fluidization of the conical bed are as follows:

1. **O→A stage**: because Ug0 is relatively low, the stagnant height of the particle bed remains unchanged as at the beginning. The total pressure drop, ΔPt, increases up to the maximum point, ΔPm*ax*, i.e. point A as shown in Fig.2. This phenomenon is the same as that observed for liquid–solid tapered beds by Peng and Fan [1], and the flow regime is also termed the fixed bed regime. The superficial gas velocity, to which point A in Fig1.2 corresponds, is called the minimum fluidized velocity, Umf.

**A→.B stage**: When Ug0 is higher than Umf as shown In Fig.2 ΔPt decreases with the increase of Ug0, and it is observed that the stagnant height of the conical bed does not change. The same phenomenon is also observed for gas–solid systems by Olazar et al. [2] and for liquid–solid systems by Peng and Fan [1]. Here, the flow regime is named a partially fluidized bed. When Ug0 reaches Ums in Fig.1.2, the characteristics of total pressure drop are different from those in the above two stages.

**B→C stage**: if Ug0 is greater than Ums, ΔPt stays nearly constant as shown in below Fig. In this stage, it is observed that slugging fluidization, bubble fluidization and spouting fluidization occur for the conical bed with cone angles of 4.61, 7.47 and 9.52°, respectively. In this stage, the characteristics of fluidization of the gas–solid conical bed are different from that of liquid–solid ones as reported by Peng and Fan [1]. Depending on the cone angle, the flow regime is called a slugging or spouting fluidization regime.

Reversing the fluidization process, the fluidized bed is defluidized by decreasing the superficial gas velocity. The same regimes are observed in below Fig1.2.

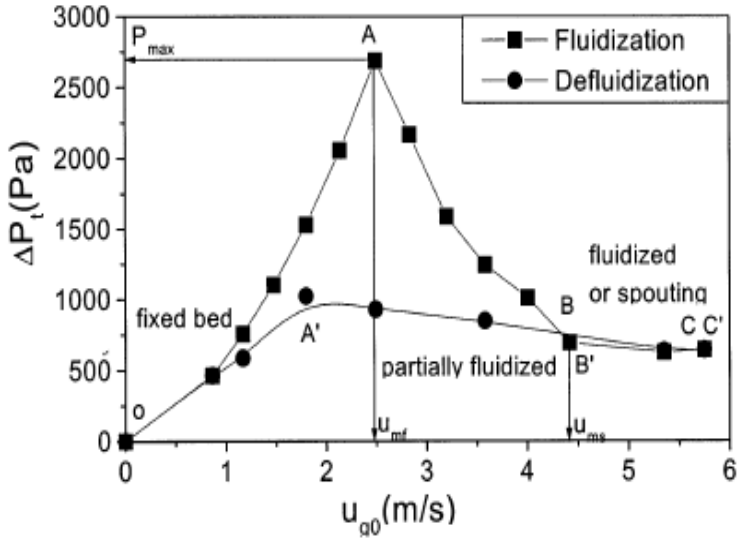


Fig.1.2 Effect of superficial gas velocity on total pressure drop

# CHAPTER 2

## LITERATURE REVIEW

# LITERATURE REVIEW

Most of the gas–solid fluidization behavior studies that have been reported are for straight cylindrical or columnar fluidized beds, although a considerable proportion of the fluidized beds have inclined walls or have a tapered bottom section. A velocity gradient exists in the axial direction, leading to unique hydrodynamic characteristics. Due to this characteristic, tapered fluidized beds have found wide applicability in many industrial processes such as, waste water treatment, immobilized biofilm reaction, incineration of waste materials, coating nuclear fuel particles, crystallization, coal gasification and liquefaction and roasting sulfide ores, food processing,etc.Tapered fluidized beds are useful for fluidization of materials with a wide particle size distribution, as well as for exothermic reactions. They can be operated smoothly without any instability,i.e. with less pressure fluctuations and also for extensive particle mixing. In spite of its advantages and usefulness, not much work has been reported in literature for understanding certain important characteristics, especially minimum fluidization velocity and maximum pressure drop. Studies have been reported by researchers to determine the factors affecting minimum fluidization velocity and maximum pressure drop. But some of these results are limited to regular particles only. Some of the previous investigations include fixed bed pressure drop calculations, flow regimes, incipient condition of fluidization, voidage distribution and bed expansion calculations and development of a model for maximum pressure drop at incipient fluidization condition of a tapered fluidized bed. The model developed by Shi et al.[7] is based on Ergun's equation and neglects friction between the particles and the wall.Biswal et al.[8,9] developed theoretical models, for minimum fluidization velocity and pressure drop in a packed bed of spherical particles for gas–solid systems in conical vessels. Due to the angled walls, random and unrestricted particle movement occurs in a tapered bed with reduced backmixing.Olazer et al.[3] compared their experimental results with that calculated using the models developed by Gelperin etal.[4] and Gorshtein and Mukhlenov[10] for maximum pressure drop and found that the predictions were not very accurate. They therefore proposed a modified equation for calculation of maximum pressure drop. Later, Peng and Fan[1] made an in-depth study of the hydrodynamic characteristics of solid–liquid fluidization in a tapered bed and derived theoretical models for the prediction of minimum fluidization velocity and maximum pressure drop, based on the dynamic balance of forces exerted on the particle. The experiments were however carried out for spherical particles only. Jing et al[11]. and Shan et al.[12]

developed models for gas–solid conical fluidized beds for spherical coarse and fine particles based on the Peng and Fan models but neglected the pressure drop due to the kinetic change in the bed. Depypere et al. [13] have carried out studies in a tapered fluidized bed reactor and proposed empirical models for determination of expanded bed height by using static pressure and wall surface temperature measurements.

Levey et al [1960] have successfully used tapered beds in chemical reactions Peng and Fan [1997] have mentioned that the beds could be used for biochemical reactions and roasting of sulfide ores. Kumar et al [1981] and Yogesh Chandra and Jagannath Rao[1981] have investigated the hydro dynamics of gas -solid fluidization in tapered vessels using single size particles.

Tapered fluidized beds have many attractive features, among which are their capabilities for handling particles with different sizes and properties ( Scott and Hancher, 1976; Ishii *et al.,* 1977) and for achieving extensive particle mixing ( Babu *et al.,* 1973), These beds have been widely applied in various processes including biological treatment of wastewater, immobilized biofilm reaction, incineration of waste materials, coating nuclear fuel particles, crystallization, coal gasification and liquefaction, and roasting sulfide ores. Interestingly, industrial fluidized beds are, more often than not, fabricated with tapered sections at the bottom.

Nevertheless, fundamental understanding of the behavior of tapered fluidized beds appears to lag far behind their applications. Some of the previous investigations include studies on pressure drop of fixed and fluidized beds in tapered vessels (Koloini and Farkas, 1973; Biswal *et al.,* 1984), flow regimes, incipient condition of fluidization,voidage distribution and bed expansion (Hsu, 1978), and particle mixing (Ridgway, 1965; Maruyama and Sato, (199l).

A fluidized bed is formed when the particles in the bed are in dynamic equilibrium; the fluid drag force and the buoyancy force are exerted in the upward direction against the gravitational force, which pulls the particles downward ( Wilhelm and Kwauk, 1948; Davidson and Harrison, 1971). This drag force is constant at any position of a columnar bed of uniform particles;

however, it decreases in the upward direction in a tapered bed accompanied by the reduction in the superficial velocity of the fluid.

Thus, the particles at the lower part of the bed will first be fluidized upon an increase in the flow rate: in contrast, those at the upper part of the bed remain static. This phenomenon of partial fluidization is peculiar to the tapered fluidized bed. Relatively little has appeared in the open literature on hydrodynamic characteristics of tapered fluidized beds; the majority of what has been published deals with flow regimes and incipient condition of fluidization. Toyohara and Kawamura (1989) have reported the flow regime of partial fluidization in a gas solid tapered bed. Descriptions have been given in Kwauk's monograph (1993) on the change of the flow regime in a gas-solid tapered bed.

The incipient condition of fluidization in a tapered bed can be predicted based on the dynamic balance of forces exerted on the particle bed. This approach was adopted by Gelperin *et al.* (1960) and Nishi (1979) for gas-solid tapered beds, and Shi *et al.* (1984) for liquid-solid tapered beds. Nevertheless, none of these works took into account the phenomenon of partial fluidization in predicting the incipient condition of fluidization and the concomitant, maximum pressure drop.

Fluidization in tapered beds have found wide applicability in many industrial processes such as, waste water treatment (Scott and Hancher, 1976), coating of nuclear fuel particles, crystallization, coal gasification and liquification and roasting of sulfide ores (Peng and Fan, 1997), coating of food powder particles (Depypere et al., 2005), etc. Tapered fluidized beds are useful for fluidization of materials with wide particle size distribution and also for exothermic reactions. It can be operated smoothly without any instability i.e. with less pressure fluctuations (Ridgway, 1965) and also for extensive particle mixing (Babu et al. 1973, Maruyama and Sato, 1991). Various techniques including introduction of baffles, operation in multistage unit and imparting vibrations have been advocated from time to time to tackle slugging problem in conventional bed. Introduction of tapered bed instead of a conventional cylindrical one is an alternative technique in gas-solid fluidization to tackle such problem. Better solid fluid mixing and improved quality of fluidization can be achieved in a tapered bed. The gradual decrease in superficial fluid mass velocity due to increase in the cross-sectional area in the upward direction

necessitates the use of continuously decreasing size particles for smooth and stable operation of such a fluidizer. Due to angled wall, random and unrestricted particle movement occurs in tapered bed thereby reducing back mixing (Singh et al, 1992). Although some information for liquid-solid system in tapered bed is available, very little work related to gas-solid fluidization in tapered bed is available. In spite of its advantages and usefulness not much work has been reported in literature for understanding certain important characteristics, especially fluctuation ratio of the bed. Some of the previous investigations include fixed bed pressure drop calculations (Koloini and Farkas, 1973), flow regimes, incipient condition of fluidization, voidage distribution and bed expansion calculations (Hsu et al, 1978).

Biswal et al. (1982, 1984, and 1985) developed correlations for fluctuation ratio in a packed bed for spherical and non-spherical particles for gas-solid system in conical vessels but have not included the effect of density of solid and the fluidizing medium. Maruyama and Koyanagi (1993) have proposed analytical methods to predict the bed expansion and pressure drop in tapered fluidized bed. Depypere et al (2005) have carried out studies in a tapered fluidized bed reactor and proposed a model for expanded bed height by the use of static pressure and wall surface temperature measurement.

Fluidization operations in cylindrical column are extensively used in process industries. But, in a number of these operations, the particles are generally not of uniform size or there may be reduction in size due to chemical reactions like combustion or gasification, or attrition. In cylindrical beds, the particle size reduction results in entrainment, limitation of operating velocity in addition to the other demerits like slugging, non-uniform fluidization generally associated with such beds. These disadvantages are overcome by use of tapered beds to conduct fluidization. This is due to the gradual reduction of superficial velocity of the fluid because of increase in cross sectional area with height. Tapered fluidized beds have found wide applicability in many industrial processes such as biological treatment of waste water, immobilized biofilm reaction, incineration of waste materials, coating nuclear fuel particles, crystallization, coal gasification and liquefaction and roasting sulfide ores, and food processing .These beds are also useful for fluidization of materials with wide particle size distribution and also for exothermic reactions.Tapered bed can also reduce back mixing of particles.

Some of the previous investigations include development of a model for maximum pressure drop at incipient fluidization condition of a tapered fluidized bed. Biswal et al. developed an analytical expression for critical fluidization velocity and pressure drop in a packed bed of spherical particles for gas-solid system in conical vessels. Olazer et al.proposed a correlation for calculation of maximum pressure drop in conical spouted bed. Later, Peng and Fan made an in-depth study of the hydrodynamic characteristics of solid-liquid fluidization in tapered bed and derived a theoretical model based on dynamic balance of forces exerted on the particle for the prediction of critical fluidization velocity and maximum pressure drop. Jing et al. and Shan et al. developed a model for gas-solid conical fluidized bed for spherical course and fine particles respectively based on Peng and Fan model but neglected the pressure drop due to kinetic change in the bed. But all of these works were for single type particles and uniform size particles in tapered or conical bed.

There have been a lot of investigations about hydrodynamic characteristics of binary mixture of particles in conventional (cylindrical) fluidized bed. There is also an investigation for multicomponent systems in cylindrical bed.

However, in general the particle are not of uniform size in the feed itself and also there may be particle size reduction during operation in fluidized beds, which can cause high elutriation loss, defluidization, segregation in size, inhomogeneous residence time in the bed. There have been no detailed studies so far in literature regarding this aspect. Very few works are reported in the literature for hydrodynamic characteristics of binary mixtures in conical beds. Hence, the study of certain important characteristics of tapered beds is essential in the operation of the beds.

The flow of fluids of single phase has occupied the attention of scientists and engineers for many years. The equations for the motion and thermal properties of single phase fluids are well-accepted and closed form solutions for specific cases are well-documented. The state of the art for multiphase flows is considerably more primitive in that the correct formulation of the governing equations is still under debate. For this reason, the study of multiphase flows represents a challenging and potentially fruitful area of endeavor. Hence there has been an increased research activity in the experimental and numerical study of multiphase flows.

Multiphase flows can be broadly classified into four groups; gas-liquid, gas-solid, liquid-solid and three-phase flows. Gas-solid flows are usually considered to be a gas flow with suspended solid particles. This category includes pneumatic transport, bubbling/circulating fluidized beds and many others. In addition, there is also a great deal of industrial interest in pure granular flows in industrial equipment such as mixers, hoppers, ball mills, and chutes.

It has been estimated that approximately $61 billion in the U.S. chemical industry is linked to particle technology. In particular, gas-solid transport is crucial in a variety of industrially important applications, ranging from fluidized-bed reactors and dryers to pneumatic conveyors and classifiers to spray dryers and coaters. In many instances the cohesive nature of a powder sample is a prime factor contributing to difficulties in proper plant operation where powder flow ability may cause, for example, channeling and defluidization in combustion/feeder systems. The Rand Corporation conducted a six-year study of 40 solids processing plants in the U.S. and Canada. Their study revealed that almost 80% of these plants experienced solids handling problems. Hence, the problems arising due to the cohesive nature of powders concern a diverse range of industries.

Despite recent advances, an understanding of the flow and characterization of cohesive gas-solid owe remains poor. Therefore, it was felt necessary to develop a generalized correlation for the calculation of minimum fluidization velocity and maximum pressure drop in a tapered fluidized bed, which are the two important characteristics of fluidization for regular and irregular particles. In this study an empirical dimensionless correlation has been developed for predicting the minimum fluidization velocity and maximum pressure drop for regular and irregular particles of gas–solid systems taking into account all the parameters, i.e., particle diameter, particle density, tapered angle, porosity and sphericity. The correlation for pressure drop however also depends upon the bed height. The applicability of the new model has been compared to that of existing models from literature.

# CHAPTER 3

## EXPERIMENTAL DETAILS

# EXPERIMENTAL SET UP

The schematic diagram of experimental setup is shown below.

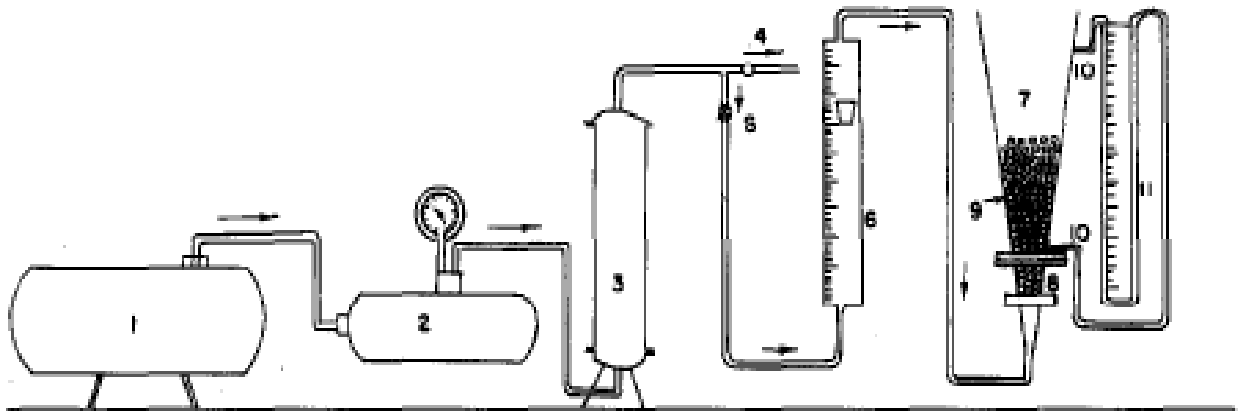


Fig 3.1 -: Experimental set-up. 1, compressor, 2 receiver, 3 silica gel tower, 4 by pass valve,5line valve, 6 rotameter, 7 conical fluidizer, 8 bed packing, 9 packing materials in fluidization state, 10 pressure tappings to manometer

## CONSTITUENTS OF EXPERIMENTAL SETUP:

The experimental set up consists of the following parts

**Air Compressor**

It is multistage air compressor of sufficient capacity.

**Air Accumulator**

It is horizontal cylinder used for storing the compressed air from compressor. There is one G.I. pipe inlet to the accumulator and one by-pass from one end of the cylinder. The exit line also at G.I line taken from the central port of the cylinder. The purpose for using air accumulator in the line is to dampen the pressure fluctuations. The accumulator is fitted with a pressure gauge; the operating pressure in the cylinder is kept at 20psig**.**

**Silica-Gel Column**

A silica gel column is provided in the line immediately after the air accumulator to arrest the moisture carried by air from the accumulator.

**Pressure Gauge**

A pressure gauge in the required range (1-50psig.)is fitted in the line for measuring the working pressure.

**Rotameter**

Rotameter is used for the measurement of flow rate of air. Two rotameters, one for the lower range (0-20 $m^3$/hr) and the other for the higher range (20-120 $m^3$/hr) were used to measure the air flow rates.

**Air Distributor**

This is an important comment of the experimental setup. It is perforated plate made up of G.I sheet. The pores of 0.5cm diameter are randomly placed in the sheet. The distributor is an integral part of calming section where it is followed by a conical section. The inside hollow space of the distributor filled with glass beads of 1.5cm outer diameter, for uniform air distribution**.**

**Conical Fluidizer**

The fluidizers consists of transport Perspex column with one end fixed to flange. The flange has 6bolt holes of 1.2cm. diameter. Two pressure tapings are provided for noting the bed pressure drop. A screen is provided in the lower flange of the fluidizer and the conical air distributor.

**Quick Opening Valve and Control Valve**

A globe valve of 1.25cm inner diameter attached to next to the pressure gauge for sudden release of the line pressure. A gate valve of 15mm inner diameter is provided in the line to control the airflow to the bed.

**Manometer Panel Board**

One set of manometer is arranged in this panel board to measure the pressure drop. Carbon tetrachloride is used as manomertic liquid .

# APPARATUS

A schematic diagram of the experimental set-up is shown in Figure3.1.The tapered columns were made of Perspex sheets to allow visual observation with different tapered angles. The inlet diameters were 48mm, 42mm and 50mm where as the outlet diameters were 132mm, 174 mm and 212 mm respectively. The reactor heights were 520 mm, 504 mm and 483 mm respectively. A 60 mesh screen at the bottom served as the support as well as the distributor. The calming section of the bed was filled with glass beads for uniform distribution of fluid. Two pressure taps, one at the entrance and the other at the exit section of the bed were provided to record the pressure drops. Pressure drop was measured by manometer, which was one meter long. Carbon tetrachloride (density=1594 kg $m^{-3}$) was used as the manometric fluid. Air at a temperature of 28 $^0$C ($\rho_f$ =1.17 kg $m^{-3}$ and $\mu_f$ =1.8*$10^{-5}$ kg $m^{-1}$ $s^{-1}$) used as the fluidizing medium was passed through a receiver and a silica gel tower to dry and control the air flow before being sent through the tapered column. Two rotameters, one for the lower range (0-20 $m^3$/hr) and the other for the higher range (20-120 $m^3$/hr) were used to measure the air flow rates.

# PROCEDURE

The experiments were carried out in tapered column having tapered angles of 4.61°, 7.47° and 9.52°. Five type of materials such as glass beads (spherical particles having density of 2600 kg/m$^3$), sago (white colored spherical cereal having density of 1303 kg/m$^3$), coal (irregular particles having density of 1600 kg/m$^3$), iron (irregular particles having density of 4400 kg/m$^3$) and dolomite (irregular particles having density of 2800 kg/m$^3$), were used for the investigation. All experimental runs were performed at a temperature of around 303 K and under 101.325 kPa pressures. The diameter of the particles was determined by sieving technique. The density of the particles was obtained by dividing the weight of the particles by the displaced water volume when the particles were placed into a cylindrical column filled with water.

A weighed amount of material was charged to the bed and air passed through it for about five minutes till the system was stable. The initial stagnant bed height was recorded. Then the velocity of the air was increased incrementally allowing sufficient time to reach a steady state. The rotameter and manometer readings were noted for each increment in flow rate and the pressure drop and superficial velocity calculated. Air flow rate was gradually increased and the corresponding bed pressure drops were measured. When the minimum fluidization was attained, the expanded static bed height was also measured. As the bed fluctuates between two limits of gas-solid fluidization, heights of the upper and the lower surfaces of the fluctuating bed were measured for each fluid velocity higher than the minimum fluidization velocity.

# CHAPTER 4

## THEORETICAL SECTION

# THEORETICAL SECTION

## Equation for total pressure drop in a fixed bed

According to the conclusions reached in Refs. [1, 6], the gas velocity distribution in the cross-section of the conical bed is uniform. Therefore, in the fixed bed regime, Ergun's equation is adopted for calculating the pressure drop.

$$-\frac{\mathrm{d}p}{\mathrm{d}h} = 150\frac{(1-\varepsilon)^2}{\varepsilon^3}\frac{\mu_{\mathrm{g}}(u_{\mathrm{g}}-u_{\mathrm{s}})}{(\phi_{\mathrm{s}}d_{\mathrm{p}})^2} + 1.75\frac{(1-\varepsilon)}{\varepsilon^3}\frac{\rho_{\mathrm{g}}(u_{\mathrm{g}}-u_{\mathrm{s}})^2}{\phi_{\mathrm{s}}d_{\mathrm{p}}} \tag{B1}$$

where $u_{\mathrm{s}} = 0$.

If the voidage remains uniform with bed height, the gas velocity, U*g*, in the conical bed, is given as

$$u_{\mathrm{g}} = \frac{u_{\mathrm{g0}}\left(r_0 + h\,\tan\frac{\alpha}{2}\right)^2}{r_0^2} \tag{B2}$$

By substituting Eq. (B2) into Eq. (B1), Ergun's equation becomes

$$-\frac{\mathrm{d}p}{\mathrm{d}h} = 150\frac{(1-\varepsilon)^2}{\varepsilon^3}\frac{\mu_{\mathrm{g}}u_{\mathrm{g0}}}{(\phi_{\mathrm{s}}d_{\mathrm{p}})^2\left[1+\frac{\tan\alpha/2}{r_0}h\right]^2} + 1.75\left(\frac{1-\varepsilon}{\varepsilon^3}\right)\frac{\rho_{\mathrm{g}}u_{\mathrm{g0}}^2}{(\phi_{\mathrm{s}}d_{\mathrm{p}})\left[1+\frac{\tan\alpha/2}{r_0}h\right]^4} \tag{B3}$$

By integrating along the bed height, the pressure drop is

$$-\Delta p_t = 150\frac{(1-\varepsilon)^2}{\varepsilon^3}\frac{\mu_g u_{g0} r_0}{(\phi_s d_p)^2 \tan\frac{\alpha}{2}}\left[1-\frac{1}{1+\frac{\tan\alpha/2}{r_0}h}\right] + 1.75\left(\frac{1-\varepsilon}{\varepsilon^3}\right) \times \frac{\rho_g r_0 u_{g0}^2}{3\phi_s d_p \tan\frac{\alpha}{2}}\left[1-\frac{1}{\left(1+\frac{\tan\alpha/2}{r_0}h\right)^3}\right] \quad \text{(B4)}$$

Where ,

$$\tan\frac{\alpha}{2} = \frac{r_1 - r_0}{h}$$

If

$$A = 150\frac{(1-\varepsilon)^2}{\varepsilon^3}\frac{\mu_g}{(\phi_s d_p)^2}$$

and

$$B = 1.75\left(\frac{1-\varepsilon}{\varepsilon^3}\right)\frac{\rho_g}{\phi_s d_p},$$

by considering Ǿs=1 in this experiment, Eq. (B4) reads

$$-\Delta p_t = A u_{g0} h\frac{r_0}{r_1} + B u_{g0}^2 h\frac{r_0(r_0^2 + r_0 r_1 + r_1^2)}{3r_1^3} \quad \text{(B5)}$$

**Condition for point A**

According to the conclusion drawn by Peng and Fan [1], the buoyancy force exerted on the entire particle bed by fluid flowing upwards equals the effective gravitational force of all particles in the bed at point A in Fig.1.2, i.e.

$$F = G \tag{C1}$$

In the fixed bed regime, the total pressure drop can be calculated by Ergun's equation as follows

$$\mathrm{d}p = (Au_{\mathrm{g}} + Bu_{\mathrm{g}}^2)\,\mathrm{d}h \tag{C2}$$

In the layer with radius *r*, the buoyancy force exerted on the particles by the fluid is

$$\mathrm{d}F = \pi r^2\,\mathrm{d}p = \pi\left[Au_{\mathrm{g0}}r_0^2 + \frac{Bu_{\mathrm{g0}}^2 r_0^4}{\left(r_0 + \tan\frac{\alpha}{2}\right)^2}\right]\mathrm{d}h \tag{C3}$$

Integration of Eq. (C3) along the height of the conical bed gives

$$F = \pi r_0^2 h\left(Au_{\mathrm{g0}} + Bu_{\mathrm{g0}}^2\frac{r_0}{r_1}\right) \tag{C4}$$

At the same time, the effective weight of particles in the layer is

$$\mathrm{d}G = (1-\varepsilon)(\rho_{\mathrm{s}} - \rho_{\mathrm{g}})g\pi r^2\,\mathrm{d}h \tag{C5}$$

Integration of Eq. (C5) along the height of the conical bed gives

$$G = (1-\varepsilon)(\rho_{\mathrm{s}} - \rho_{\mathrm{g}})g\pi r_0^2 h\frac{r_1^2 + r_0 r_1 + r_0^2}{3r_0^2} \tag{C6}$$

According to Eq. (C1), the following equation is obtained for calculating the minimum fluidization velocity, Umf

$$B\frac{r_0}{r_1}u_{\mathrm{mf}}^2 + Au_{\mathrm{mf}} - (1-\varepsilon)(\rho_{\mathrm{s}} - \rho_{\mathrm{g}})g\frac{r_1^2 + r_1 r_0 + r_0^2}{3r_0^2} = 0 \qquad \text{(C7)}$$

The total pressure drop, ΔPt, is also calculated by substituting Umf into Eq. (B5).

**Condition for point B**

According to the conclusion drawn by Peng and Fan [1], the fully fluidized bed occurs when the buoyancy force exerted on the particles in the top layer by fluid
flowing upwards equals the effective gravitational force in the layer at point B in Fig. A1.2, i.e.

$$\mathrm{d}F = \mathrm{d}G \qquad \text{(D1)}$$

By combing Eq. (C3) with Eq. (C5), the following equation is derived

$$A\left(\frac{r_0}{r_1}\right)^2 u_{\mathrm{ms}} + B\left(\frac{r_0}{r_1}\right)^4 u_{\mathrm{ms}} - (1-\varepsilon)(\rho_{\mathrm{s}} - \rho_{\mathrm{g}})g = 0 \qquad \text{(D2)}$$

The spouting velocity is calculated by solving Eq. (D2). Here, according to the definition of fluidization, the pressure gradient, dP*t*/d*h*, should be equal to Psg.

# CHAPTER 5

## EXPERIMENTAL OBSERVATIONS

## EFFECT OF CONE ANGLE

The fig.5.1 shows the effect of the cone angle of the conical bed on flow regimes, where the bed cone angles are 4.61, 7.47 and 9.52° and the stagnant height of the conical bed is 0.195 m. It can be seen from Fig.4 that there are three regimes for different cone angles, but the maximum pressure drop, ΔPmax, the minimum fluidization velocity, Umf, the spouting pressure drop, ΔPsp, and the spouting velocity, Ums, increase with the increase of cone angle. When Ug0 exceeds Ums, it is observed that for a cone angle of 4.61°, fluidization suddenly occurs and that pulsing slugging follows directly, while for a cone angle of 7.47°, only bubble fluidization happens. For the cone angle of 9.52°, only the particles in the center of the conical bed flow upward and form a 'fountain', but the particles near the wall flow downward. Therefore, the motion of particles for the conical bed with a cone angle of 9.52° seems to be similar to conventional spouting

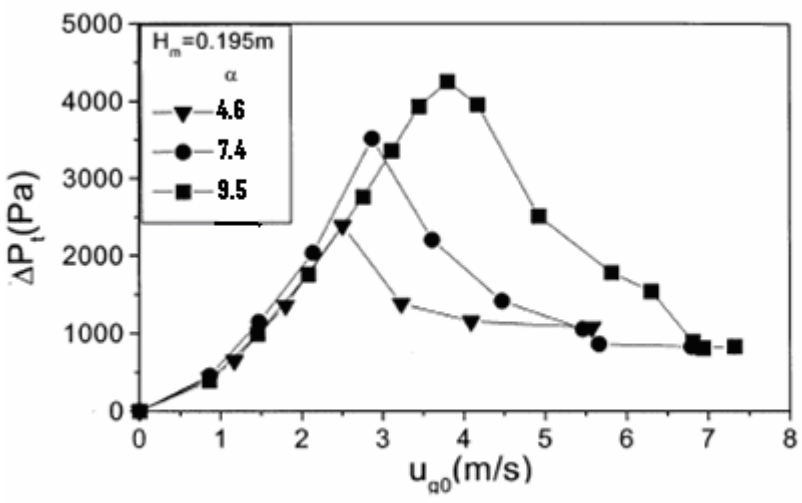


fig.5.1 effect of cone angles of fluidization in conical bed

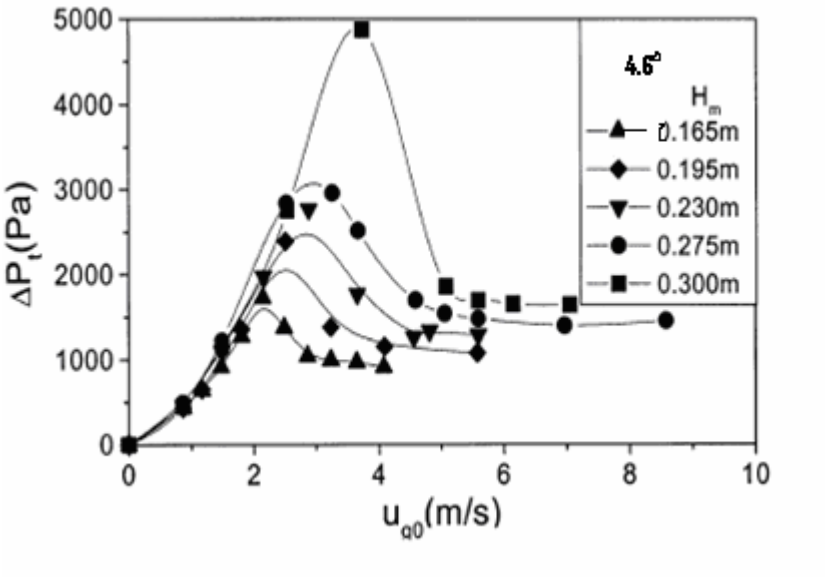


Fig.5.2 Effect of stagnant bed height of the conical bed on fluidization

## EFFECT OF STAGNANT HEIGHT

The above fig shows the effect of the stagnant height of the conical bed on flow regime in the case of a bed cone angle of 4.6°. It can be seen from Fig. 5.2 that there are three regimes, and the values of ΔPmax, Umf, ΔPsp, and Ums increase with increasing stagnant bed height.

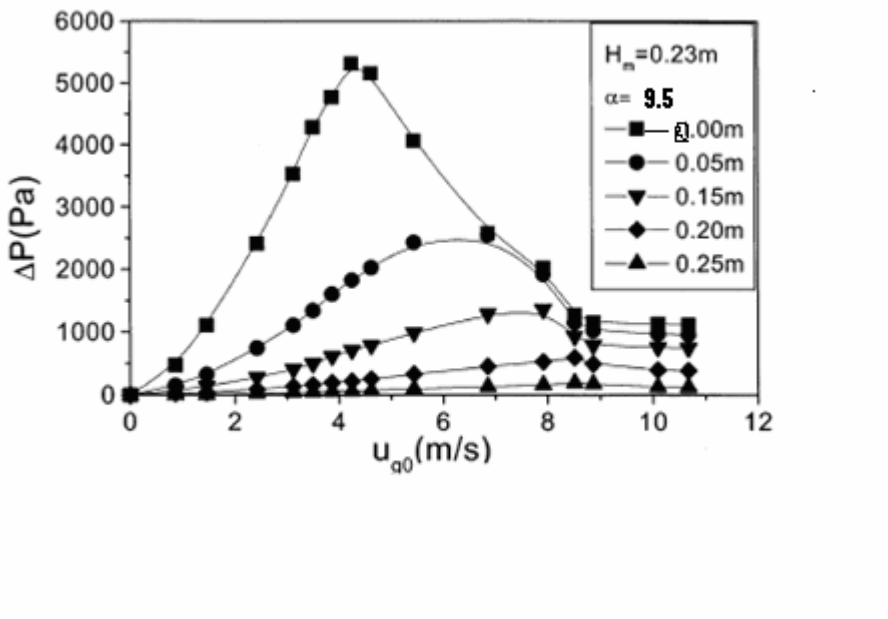


Fig.5.3 pressure drop at different position along the bed height

## LOCAL CHARACTERISTICS

The above fig., shows the local pressure drop along the height of the conical bed wall with increasing Ug0 when the cone angle and stagnant height are 9.52° and 0.23 m, respectively. It can be seen that the profile of local pressure drop shows the same tendency as that of the total pressure drop with increasing Ug0. By moving to a higher position in the bed, the local pressure drop decreases because the cross-sectional area increases, but the local minimum fluidization velocity, Umfl, to which the maximum local pressure drop corresponds, increases as shown in above Fig5.3. It is also seen that the local spouting velocity, Umsl, does not change with variation in the bed height. From the above experimental results of local pressure drop versus Ug0, it is concluded that when Ug0 is less than Ums, the particles in the upper section of the bed are not fluidized and the particles above restrict the bed expansion in the lower section. In this case the conical bed is in the partial fluidization regime. When Ug0 is greater than Ums, the condition of non-fluidization disappears.

# CHAPTER 6

## PREVIOUSLY DEVELOPED CORRELATIONS

## FOR CONVENTIONAL BEDS

**Developed correlations For Fluctuation Ratio (For Irregular Particle Mixture) are:**

(1) Un-Promoted Bed

$$r = 4.6\left[\left(\frac{dp}{Dc}\right)^{0.00812}\left(\frac{Dc}{Hs}\right)^{-0.1035}\left(\frac{\rho_s}{\rho_f}\right)^{-0.02}\left(\frac{U-U_{mf}}{U_{mf}}\right)^{1.1036}\right]$$

(2) Disc Promoted Bed without Stirring Effect

$$r = 4.3\left[\left(\frac{dp}{De}\right)^{0.0323}\left(\frac{Dc}{Hs}\right)^{-0.0846}\left(\frac{\rho_s}{\rho_f}\right)^{-0.0346}\left(\frac{U-U_{mf}}{U_{mf}}\right)^{1.215}\right]$$

(3)Rod Promoted Bed without Stirring Effect

$$r = 2.97\left[\left(\frac{dp}{De}\right)^{0.003}\left(\frac{Dc}{Hs}\right)^{-0.072}\left(\frac{\rho_s}{\rho_f}\right)^{-0.2826}\left(\frac{U-U_{mf}}{U_{mf}}\right)^{1.061}\right]$$

(4)Disc Promoted Bed with Stirring Effect

$$r = 2.22\left[\left(\frac{dp}{De}\right)^{-0.106}\left(\frac{Dc}{Hs}\right)^{-0.414}\left(\frac{\rho_s}{\rho_f}\right)^{0.24}\left(\frac{U-U_{mf}}{U_{mf}}\right)^{1.312}\right]$$

(5)Rod Promoted Bed with Stirring Effect

$$r = 2.82\left[\left(\frac{dp}{De}\right)^{0.02}\left(\frac{Dc}{Hs}\right)^{-0.1589}\left(\frac{\rho_s}{\rho_f}\right)^{0.366}\left(\frac{U-U_{mf}}{U_{mf}}\right)^{1.08}\right]$$

**Developed correlations For Expansion Ratio are:**

(6)Un-Promoted Bed

$$R = 2.34\left[\left(\frac{dp}{Dc}\right)^{-0.0155}\left(\frac{Dc}{Hs}\right)^{-0.056}\left(\frac{\rho_s}{\rho_f}\right)^{-0.702}\left(\frac{U-U_{mf}}{U_{mf}}\right)^{0.89}\right]$$

(7)Disc Promoted Bed without Stirring Effect

$$R = 1.45\left[\left(\frac{dp}{De}\right)^{0.0337}\left(\frac{Dc}{Hs}\right)^{-0.2773}\left(\frac{\rho_s}{\rho_f}\right)^{0.02}\left(\frac{U-U_{mf}}{U_{mf}}\right)^{0.756}\right]$$

(8)Rod Promoted Bed without Stirring Effect

$$R = 1.274\left[\left(\frac{dp}{De}\right)^{0.036}\left(\frac{Dc}{Hs}\right)^{-0.4064}\left(\frac{\rho_s}{\rho_f}\right)^{0.0223}\left(\frac{U-U_{mf}}{U_{mf}}\right)^{1.077}\right]$$

(9)Disc Promoted Bed with Stirring Effect

$$R = 1.5\left[\left(\frac{dp}{De}\right)^{0.0682}\left(\frac{Dc}{Hs}\right)^{-0.153}\left(\frac{\rho_s}{\rho_f}\right)^{0.589}\left(\frac{U-U_{mf}}{U_{mf}}\right)^{0.96}\right]$$

(10) Rod Promoted Bed with Stirring Effect

$$R = 1.49\left[\left(\frac{dp}{De}\right)^{0.011}\left(\frac{Dc}{Hs}\right)^{0.0125}\left(\frac{\rho_s}{\rho_f}\right)^{-0.677}\left(\frac{U-U_{mf}}{U_{mf}}\right)^{1.088}\right]$$

## FOR TAPERED BEDS

Some of the well known correlations available for predicting the minimum fluidization velocity (*U*mf) and maximum pressure drop (_*P*max) for tapered beds are those by **Peng and Fan** [1] and **Jing et al**. [11]. **Peng and Fan** [1] developed a model for estimating minimum fluidization velocity and maximum pressure drop for solid–liquid system and spherical particles based on the dynamic balance of forces exerted on the particle. The correlation reported by them for minimum fluidization velocity is given in Eq. (1).

$$C_1 U_{mf} + C_2 \left(\frac{D_0}{D_1}\right) U_{mf}^2 - (1-\varepsilon_0)(\rho_s - \rho_f) g \times \frac{(D_0^2 + D_0 D_1 + D_1^2)}{3 D_0^2} = 0 \quad (1)$$

The equation for pressure drop has been developed from Ergun's equation, which also includes the pressure drop due to a kinetic energy change in the bed:

$$-\Delta P_{max} = C_1 H_s \frac{D_0}{D_1} U_0 + C_2 H_s \frac{D_0 (D_0^2 + D_0 D_1 + D_1^2)}{3 {D_0}^2} U_0^2 + \frac{1}{2}\left(\frac{U_0}{\varepsilon_0}\right)^2 \left[\left(\frac{D_0}{D_1}\right)^4 - 1\right] \rho_f \quad (2)$$

**Jing et al.** [11] developed a model based on Ergun's equation for pressure drop calculation but neglecting the pressure drop due to the kinetic energy change in the bed. The equation proposed by them for nearly spherical particles is

(3)

$$-\Delta P_t = C_1 U_0 H_s \frac{r_0}{r_1} + C_2 U_0^2 H_s \frac{r_0 (r_0^2 + r_0 r_1 + r_1^2)}{3 r_1^2}$$

Recently, **Sau et.al. (**2007) developed a correlation for maximum pressure drop in gas–solid tapered fluidized beds

$$\mathrm{Fr} = 0.2714(\mathrm{Ar})^{0.3197}(\sin\alpha)^{0.6092}\left(\frac{\varepsilon_0}{\emptyset_s}\right)^{-0.6108} \tag{4}$$

$$\Delta P_{\max} = 7.457\left(\frac{D_1}{D_0}\right)^{0.038}\left(\frac{d_p}{D_0}\right)^{0.222}\left(\frac{H_s}{D_0}\right)^{0.642}\left(\frac{\rho_s}{\rho_f}\right)^{0.723} \tag{5}$$

On the basis of Ergun's equation and Baskakov and Gelperm's modification [4] forcone geometry, a packed bed pressure drop equation for conical beds was developed by **Biswal.et.al.(**1984), for gas-solid systems,

$$\Delta P_c = \cos\frac{\alpha}{2}\left\{37\ 17(\tan\alpha)^{-0\ 47}\frac{\mu(1-\epsilon_{pa})^2}{g_c d_p{}^2\epsilon_{pa}}\times \times\frac{R_0}{R}(R-R_0)V_0 + 0.75\frac{\rho_f(1-\epsilon_{pa})}{g_c d_p\epsilon_{pa}{}^3}\times \times\frac{R_0}{3R^3}(R^3-R_0{}^3)V_0{}^2\right\} \tag{6}$$

at the onset of fluidization,

$$\Delta P_{mf} = \cos\frac{\alpha}{2}\left\{37\ 17(\tan\alpha)^{-0\ 47}\frac{\mu(1-\epsilon_{pa})^2}{g_c d_p{}^2\epsilon_{pa}}\times \times\frac{R_0}{R}(R-R_0)V_{0mf} + 0.75\frac{\rho_f(1-\epsilon_{pa})}{g_c d_p\epsilon_{pa}{}^3}\times \times\frac{R_0}{3R^3}(R^3-R_0{}^3)V_0{}^2\right\} \tag{7}$$

$\Delta P_{mf}$ may also be written as

$$\Delta P_{mf} = R_{mf}(1-\epsilon_{mf})(\rho_p-\rho_f)$$

A correlation for fluctuation ratio in conical vessels for regular particle has been developed by **Biswal et al** (1984) using dimensional analysis approach based on four dimensionless groups neglecting the effect of density of gas and solid particles. The correlation reported by Biswal et al (1984) for fluctuation ratio of regular particle is given in equation (8) and for irregular particle is in equation (9).In equation (9) the effect of top diameter has also been neglected.

$$r = 3.168\left(\frac{D_c}{h_s}\right)^{-0.16}\left(\frac{h_s}{D_0}\right)^{-0.24}\left(\frac{d_p}{D_0}\right)^{0.14}\left(\frac{G_f - G_{mf}}{G_{mf}}\right)^{0.17} \tag{8}$$

$$r = 9.48\left(\frac{D_c}{h_s}\right)^{-0.83}\left(\frac{d_p}{D_0}\right)^{0.27}\left(\frac{G_f - G_{mf}}{G_{mf}}\right)^{0.32}\left(\frac{\rho_s}{\rho_f}\right)^{-0.15} \tag{9}$$

Semi-empirical correlation for *u*ms is given by **Bi et al.** [17] as follows:

$$(\mathrm{Re}_0)_{\mathrm{ms}} = 0.202\sqrt{\mathrm{Ar}(D_1/D_0)((D_1/D_0)^2 + (D_1/D_0) + 1)/3} \tag{10}$$

Where

where $(\mathrm{Re}_0)_{\mathrm{ms}} = (u_{\mathrm{ms}} d_{\mathrm{p}} \rho_{\mathrm{g}})/\mu_{\mathrm{g}}$ and $\mathrm{Ar} = g d_{\mathrm{p}}^3(\rho_s - \rho_{\mathrm{g}})\rho_{\mathrm{g}}/\mu_{\mathrm{g}}^2$.

For the conventional spouting bed, an empirical correlation was given by **Mathur and Gishler** as:

$$u_{\mathrm{ms}} = \frac{d_{\mathrm{p}}}{D_{\mathrm{t}}}\left(\frac{D_{\mathrm{i}}}{D_{\mathrm{t}}}\right)^{1/3}\left(\frac{D_1}{D_{\mathrm{i}}}\right)^2\sqrt{\frac{2gH_{\mathrm{m}}(\rho_s - \rho_{\mathrm{g}})}{\rho_{\mathrm{g}}}} \tag{11}$$

the value of *u*ms is based on the cross-sectional area at the bottom of the fluidized bed.

# CHAPTER 7

## DEVELOPMENT OF MODELS

## DEVELOPMENT OF MODELS

Based on the experimental data obtained in the present study for different mixture of materials, correlations have been obtained by carrying out dimensionless analysis and estimating the constant coefficients by non-linear regression. In our correlations we have included the effect of tapered angle which is the most important parameter in tapered bed hydrodynamics. The proposed correlations consists of experimental systems corresponding to a wide range of geometric factors of the bed (tapered angle, gas inlet diameter) and a wide range of experimental conditions (particle size, particle density, stagnant bed height). The dimensionless correlation for (mixture of regular particles) critical fluidization velocity is given in equation (1) and for maximum pressure drop is in equation (2).

$$\mathrm{Re}_c = 16.364\left(Ar\right)^{0.1969}\left(\frac{\Delta\rho}{\rho_f}\right)^{0.3154}\left(\frac{dp_m}{D_0}\right)^{1.1854}\left(Sin\alpha\right)^{0.0585} \tag{1}$$

$$\frac{\Delta P_{\max}}{g\rho_{sm}H_s} = 0.081(Ar)^{0.1493}\left(\frac{H_s}{D_0}\right)^{-0.2337}(Sin\alpha)^{0.3826} \tag{2}$$

In order to develop correlations for binary systems, it is necessary to define the particle diameter and the density of the binary systems. In this study, they are defined as in Goossens et al. [23].

$$\frac{1}{\rho_{sm}} = \frac{w_l}{\rho_{sl}} + \frac{w_h}{\rho_{sh}} \tag{3}$$

$$\frac{1}{dp_m\rho_{sm}} = \frac{w_l}{dp_l\rho_{sl}} + \frac{w_h}{dp_h\rho_{sh}} \tag{4}$$

The dimensionless correlation for critical fluidization velocity of mixture of irregular particles is given in equation (5) and for maximum pressure drop is in equation (6).

$$\mathrm{Re}_c = 301.416\left(Ar\right)^{0.1272}\left(\frac{\Delta\rho}{\rho_f}\right)^{0.3057}\left(\frac{dp_m}{D_0}\right)^{1.562}\left(Sin\alpha\right)^{0.1919} \tag{5}$$

$$\frac{\Delta P_{\max}}{\rho_{sm}gH_s} = 0.0204(Ar)^{0.2009}\left(\frac{H_s}{D_0}\right)^{-0.2273}\left(Sin\alpha\right)^{0.2947} \tag{6}$$

# CHAPTER 8

## INTRODUCTION TO COMPUTAIONAL FLUID DYNAMICS (CFD)

## 8.1 INTRODUCTION TO CFD

The flow of fluids of single phase has occupied the attention of scientists and engineers for many years. The equations for the motion and thermal properties of single phase fluids are well accepted and closed form solutions for specific cases are well documented. The state of the art for multi phase flows is considerably more primitive in that the correct formulation of the governing equations is still under debate. For this reason the study of multiphase flows represents a challenging and potentially fruitful area of endeavor. Hence there has been an increased research activity in the experimental and numerical study of multi phase flows. Multi phase flows can be broadly classified into four groups; gas-liquid, gas-solid, liquid-solid and three phase flows. Gas-solid flows are usually considered to be a gas flow with suspended solid particles. This category includes pneumatic transport, bubbling/circulating fluidized beds and many others. In addition, there is also great deal of industrial interest in pure granular flows in equipment such as mixers ball mills and hoppers.

Various research groups to understand the gas- solid flow dynamics are conducting theoretical experimental and numerical studies. Hydrodynamics modeling of gas – solid flows has been undertaken in one form or another for over forty years now. Fluidized beds are widely used in the chemical industries. They facilitate a large variety of operations ranging from coal gasification , coating metals objects with plastics drying of solids adsorption synthesis reactions, cracking of hydrocarbons and mixing etc. This variety of processes results in a large variety of fluidized bed reactors . In gas solid contact systems, gas bubble coalesces and grows as they rise and in a deep enough bed of small diameter they may eventually become large enough to spread across the vessel. The compelling advantage of the fluidized beds such as the smooth and liquid like flow of particles allows a continuous automatically controlled operation with easy handling and rapid mixing solids etc. of small economy fluidized as contacting has been responsible for its successful use in industrial operations but such success depends on understanding and overcoming its disadvantages. Currently here are two approaches for the numerical calculation of multiphase flows, the Euler- Lagrange approach and the Euler Euler approach.

In the Euler- Lagrange, the fluid phase is treated as a continuum by solving the time averaged Navier stokes equation, while the dispersed phase is solved by tracking a large number of particles (or bubbles, droplets) through the calculated flow field. The dispersed phase can

exchange momentum, mass and energy with the fluid phase. A fundamental assumption made in this approach is that the dispersed second occupies a lower volume fraction.

In the euler-euler approaches, the different phase are treated mathematically as inter penetrating continua. Since the volume of a phase cannot be occupied by another phase, the concept of the phase volume fraction is introduced. These volume fractions are assumed to be continuous fraction of time and space and their sum is equal to 1. For granular flows, such as flow in rising fluidized bed and other suspension systems, the eulerian multiphase model is always the first choice and also for simulations in this research.

### Assumptions

1) No mass transfer between the gas phase and solid phase.
2) External body force, lift force as well as virtual mass force are ignored.
3) Pressure gradient at fully fluidized condition is constant.
4) Density of each phase is constant.

## 8.2 What is CFD (Computational Fluid Dynamics)

CFD is predicting what will happen, quantitatively, when fluid flows, often with the complication of

- Simultaneous flow of heat
- Mass transfer(e.g. )
- Phase change(e.g. melting, freezing)
- Chemical reactions(e.g. combustion)
- Mechanical movement( e.g. piston ,fans)
- Stress & displacement

### 8.2.1 Advantages of CFD

1. Able to model physical fluid phenomenon that cannot easily be simulated or measured with a physical experiment. e.g. weather system.
2. Able to model & investigate physical fluid systems more cost effectively and more rapidly than with experimental procedures. e.g. hypersonic aerospace vehicle.

### 8.2.2 Uses of CFD

1. Chemical engg. : to maintain yield from reactor and processing equipments.
2. Civil engg. : in creation of dams and aquaducts on quality and quantity of water supply
3. Mechanical engg. : in design of pumps
4. Electrical engg. : in power plant design to attain maximum efficiency
5. Aeronautical engg. : in design of aircrafts

### 8.2.3 Working Principle

1. CFD first builds a computational model that represent a system or a device and that you want to study.
2. The geometry of interest is then divided or discreted into a number of computational cells called grids or mesh.
   Discretization is the method of approximating the different equations by a system of algebraic equations for the variables at some set of discrete locations in space and time. The discrete locations are referred to as grids or mesh
3. The governing equation such as Navier stokes equation ,continuity equation and energy equations etc are discretized at each grid point using numerical analysis

- Finite difference method,
- Finite element method,
- Finite volume method

4. The discretized algebra equations are then solved at each grid points by iterative means until a converged solution is obtained.

5. The values at other point are determined by interpolating the values between the grid points.

## 8.3 CFD Goals:

CFD can assist the design and optimization of new and existing processes and products. CFD can also be used for reducing energy costs, improving environmental performance and increasing productivity and profit margins. There are many potential applications of CFD in chemical processes where predicting the characteristics of fluid flow are important. A concerned effort by industry in partnership with government and academia is needed to make similar advances in CFD possible for the chemical and other low temperature process industries.

## 8.4 Current Industrial Applications:

CFD is routinely used today in a wide variety of disciplines and industries, including aerospace, automotive, power generation, chemical manufacturing, polymer processing, petroleum exploration, medical research, meteorology and astrophysics. The use of CFD in the process industry has led to reduction in the cost of product and process development and optimization activities ( by reducing down time), reduce the need for physical experimentation, shortened time to market, improved design reliability, increased conversions and yields and facilitated the resolution of environmental, health and right to operate issues . It follows that the economic benefit of using CFD has been substantial, although detailed economic analysis are rarely reported.CFD has an enormous potential impact on industry because the solution of equations of motion provides everything that is meaningful to know about the domain. For example, chemical engineers commonly make assumptions about the fluid mechanics in process units and piping that lead to great simplifications in the equations of motion. An agitated chemical reactor may be designed on the assumption that the material in the vessel is perfectly mixed, when, in reality, it is probably not perfectly mixed. Consequently, the fluid mechanics may limit the reaction rather than the reaction kinetics and the design may be inadequate. CFD allows one to stimulate the reactor without making any assumptions about the macroscopic flow pattern and thus to design the vessel properly the first time.

# CHAPTER 9

## MODELING & SIMULATION OF CONICAL BED

## 9.1 WORKING PROCEDURE

### 9.1.1 Gambit (CFD Preprocessor)

It is a software package designed to help analyst and designers build and mesh models for CFD and other scientific applications.

The Gambit graphical user interface makes the basic steps of:

1. Building.
2. Meshing,
3. Assigning zones type to a model

Gambit has following advantages:

1. Ease of use: It is user friendly
2. CAD/CAE Integration: Gambit can import geometry from any CAD/CAE software
3. Fast Modeling: It provides a concise and powerful set of solid modeling based geometry tools
4. CAD cleanup: Gambit's semiautomatic cleanup tools can be used to repair and prepare the geometry for high quality meshing.
5. Intelligent Meshing: Different CFD problems require different mesh types. Gambit provides a wide variety of meshing tools.

**Step 1** : **Building the geometry**

There are two approaches to build the geometry

- Top Down
- Bottom Up

Top Down : construct the geometry by creating volumes ( bricks, cylinder etc ) and then multiplying them through boolean operation.

Bottom Up : create vertices, then creating edges from vertices, then connect the edges to create faces and then connect the faces to create volume.

**Step 2: Meshing the model**

Meshing can be done in different ways:

- Triangular, quadrilateral, hexahedral, tetrahedral, prism etc.
- Structured and unstructured mesh.

**Step 3: Specifying zones type**

Zone type specification defines the physical and operational characteristics of the model at its boundaries and within specific region of its domain. There are two classes of zone type specification

- Boundary type
- continuum type

Boundary type -:

In this type specifications, such as well, vent or inlet, define the characteristics of the model at its external or internal boundaries.

Continuum type -:

In this type specification, such as fluid or solid, define the characteristics of the model within specified regions of its domain. e.g. if you assign a fluid continuum type specification to a volume entity, the model is defined such that equations of momentum, continuity and species transport apply at mesh nodes or cells that exist within the volume. Conversely if you assign a solid continuum type specification to a volume entity, only the energy and species transport equations (without convection) apply at the mesh nodes or cells that exist within the volume.

Fluid zone = group of cells for which all active equations are solved.

Solid zone = group of cells for which only heat conduction problem solved.

No flow equations solved.

**9.1.2Solver**

**Steps Involved in FLUENT**

**1)** Launch Fluent and select solver 2D

**2)** Read the case file .

**3)** Define Models (Solver Properties)

a) Select segregated,2D, implicit,1st order , unsteady , absolute, cell based, Superficial Velocity from Solver.

b) Enable the Eulerian multiphase model with 2 phases.

c) Select the laminar model.

d) Define the operating conditions, turn on the gravity and set the gravitational acceleration in the negative y direction, also give the reference pressure location.

**4)** Define Materials

a) Select air as the primary phase and specify its density.

b) Define a new fluid material( the glass beads) for the granular phase and specify its density.

**5)** Define Phases

a) Specify air as the primary phase

b) Specify glass beads or any solids as the secondary phase, select granular model and specify the diameter and volume fraction of solids, Select the interphase interaction .

**6)** Boundary condition declaration

a) Set conditions at velocity inlet with specifying the velocity magnitude at

b) inlet for primary phase and for secondary phase keep the default value zero for velocity magnitude.

c) Set the boundary conditions for the pressure outlet for mixture and both

phases.

d) Set the conditions for the wall for mixture and both phases.

**7)** Solution parameter setting

a) Set the under relaxation factor for pressure, momentum and volume fraction of solids.

b) Enable the plotting of residuals during the calculation.

c) Initialize the solution.

d) Define an adaption register for the lower half of the fluidized bed.

e) Set a time step size and number of time steps for iteration, save the case and data files.

### 9.1.3Post Processing

**1)** Select phase and volume fraction of the solids in the contours, we can see the contours of solids at each instant.

**2)** Similar step is followed for displaying contours of static pressure of mixture.

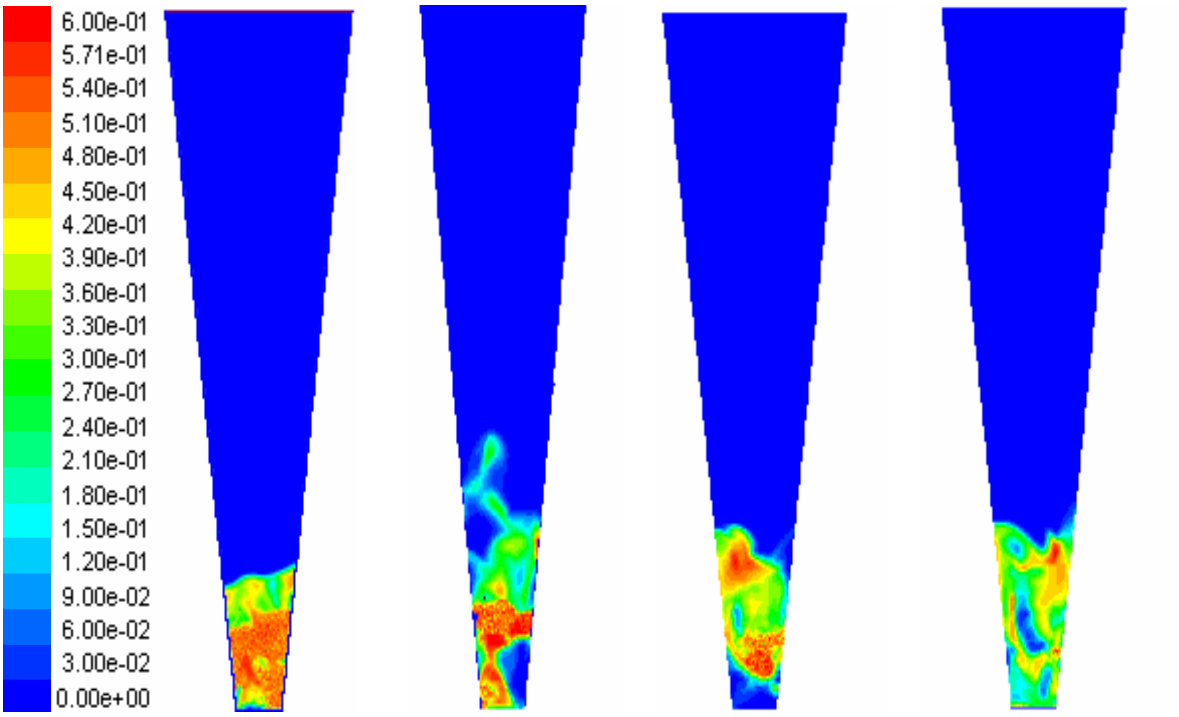


Fig 7)-: **Contours of Solid(iron) Fraction for Bed height =5.6 cm (Particle Size = 0.00158 m) at different flowrates after 1 second**

# CHAPTER 10

## RESULTS AND DISCUSSION

## RESULTS AND DISCUSSION

The hydrodynamic behavior of fluidization in tapered beds is best described by the plot of pressure drop across the bed versus superficial velocity of the fluid at the entrance. Such a plot is shown in Figure 8. From point A to point B, the pressure drop increases with the increase of superficial gas velocity. The transition from fixed bed to partially fluidized bed occurs at point B. From point B, the pressure drop decreases with the increase of superficial gas velocity and from point C it remains constant. Point B to point C is called partially fluidized bed and thereafter it is called fully fluidized bed. The hydrodynamic characteristics associated with the phenomenon are critical fluidization velocity, maximum pressure drop, critical velocity for full fluidization, pressure drop at full fluidization, maximum velocity for full defluidization and hysteresis.The details and the significance of each of the characteristics is explained by Peng and Fan [1].The velocity at point B is called critical fluidization velocity or minimum velocity for partial fluidization. At this point the pressure drop was maximum.

The critical fluidization velocity and maximum pressure drop were calculated using equation (1) and (2) respectively for binary mixture of regular particles and using equation (3) and (4) respectively for homogeneous binary mixture of irregular particles in gas-solid system and compared with experimental data.

The predicted critical fluidization velocity and maximum pressure drop with experimental results are shown in figure 9 and figure 10, 11, 12 respectively for regular particles and figure14,15,16,17 respectively for irregular particles .The average absolute percentage errors for critical fluidization velocity and maximum pressure drop is within 10%. All figures show good agreement between the predicted values and the experimental data. Comparison of critical fluidization velocity and maximum bed pressure drop with experimental results in absolute error (%) are shown in Table 2, 3 and 4, 5. It was also experimentally seen that the $U_c$ was not a function of stagnant bed height in tapered bed. This phenomenon was also observed by Povrenovic et al. [24] and Caicedo et al. [25].The critical fluidization velocity of homogeneous binary mixture of irregular particles is strongly dependent upon the ratio of $\left(\frac{dp_m}{D_0}\right)$ compared to other parameters whereas the maximum pressure drop is strongly dependent upon bed aspect ratio $\left(\frac{H_s}{D_0}\right)$.This can also seen in Table4 and 5.

# CHAPTER 11

## CONCLUSION

## CONCLUSION

The hydrodynamic features of the tapered fluidized bed are very different from those of the columnar fluidized bed; therefore, the known relations for the columnar bed cannot be used in calculating those for the tapered bed. Correlations have been developed for the calculation of critical fluidization velocity and maximum bed pressure drop for binary mixture of regular and irregular particles in gas-solid system in tapered beds. The experimental values for gas-solid systems in tapered beds were found to fit well with the proposed correlations. This indicates that the proposed correlations is valid and are of practical use. Though the average absolute percentage errors are within 10%, but some cases (table 2 and table 3) the absolute errors are slightly high. This needs more work to improve upon the correlations and to minimize the errors. The proposed correlations could find practical utility in designing and operation of tapered fluidized beds for various gas- solid systems.

# NOMENCLATURE

$D_0$ bottom diameter of tapered bed, m.

$D_1$ top diameter of tapered bed, m.

Dc mean diameter of cone, m

$d_p$ particle diameter, m.

$h_s$ initial static height of the particle bed, m.

U superficial velocity of the fluidizing fluid, m/s.

$U_{mf}$ minimum fluidization velocity based on bottom diameter of the bed, m/sec.

$G_f$ mass velocity of fluid at fluidization condition, kg/m-hr

$G_{mf}$ mass velocity of fluid at minimum fluidization condition, kg/m-hr

r fluctuation ratio, dimensionless

g gravity ,$ms^{-2}$

dpm particle diameter of binary mixture ,m

dpl diameter of light particle , m

dph diameter of heavy particle , m

Hs initial stagnant height of the particle bed, m

$\Delta\rho$ $\rho_{sm} - \rho_f$

$U_c$ critical fluidization velocity based on the diameter of entrance of the bed ,$ms^{-1}$

$\Delta P_{max}$ maximum pressure drop through the particle bed (Pa)

Ar Archimedes number, $(= g d_{pm}^{\,3} \rho_{sm}^{\,2} / \mu_f^{\,2})$

$Re_c$ Reynolds number at Uc, $(= dp_m U_c \rho_f / \mu_f)$

$w_l$ weight fraction of light (or small) particle

$w_h$ weight fraction of heavy (or big) particle

**Greek letters**

$\rho_f$ fluid density, $kg/m^3$

$\alpha$ tapered angle, deg

$\mu_f$ fluid viscosity, kg $m^{-1}$ $s^{-1}$

$\rho_{sm}$ density of binary mixture, kg $m^{-3}$

$\rho_{sl}$ density of light(small) particle, kg $m^{-3}$

$\rho_s$ solid density, kg/$m^3$

$\rho_{sh}$ density of heavy(big) particle, kg $m^{-3}$

**Subscript**

exp. experimental value

GB1 glass bead of size 2608 $\mu$m

GB2 glass bead of size 2215 $\mu$m

S1 sago of size 2608 $\mu$m

S2 sago of size 2215 $\mu$m

C1 coal of size 1718 $\mu$m

C2 coal of size 1303 $\mu$m

I1 iron ore of size 1718 $\mu$m

I2 iron ore of size 1303 $\mu$m

D1 dolomite of size 1718 $\mu$m

D2 dolomite of size 1303 $\mu$m

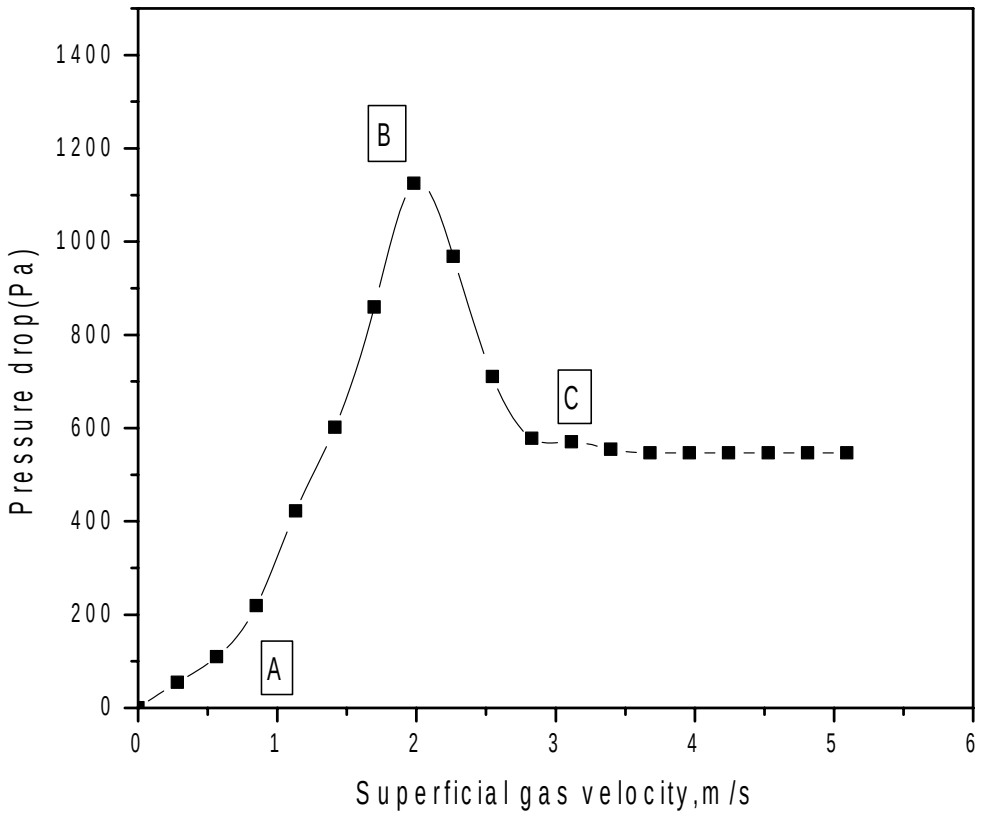
Pressure drop(Pa)
1400
1200
1000
800
600
400
200
0
0
1
2
3
4
5
6
Superficial gas velocity,m/s
A
B
C

Figure-8.

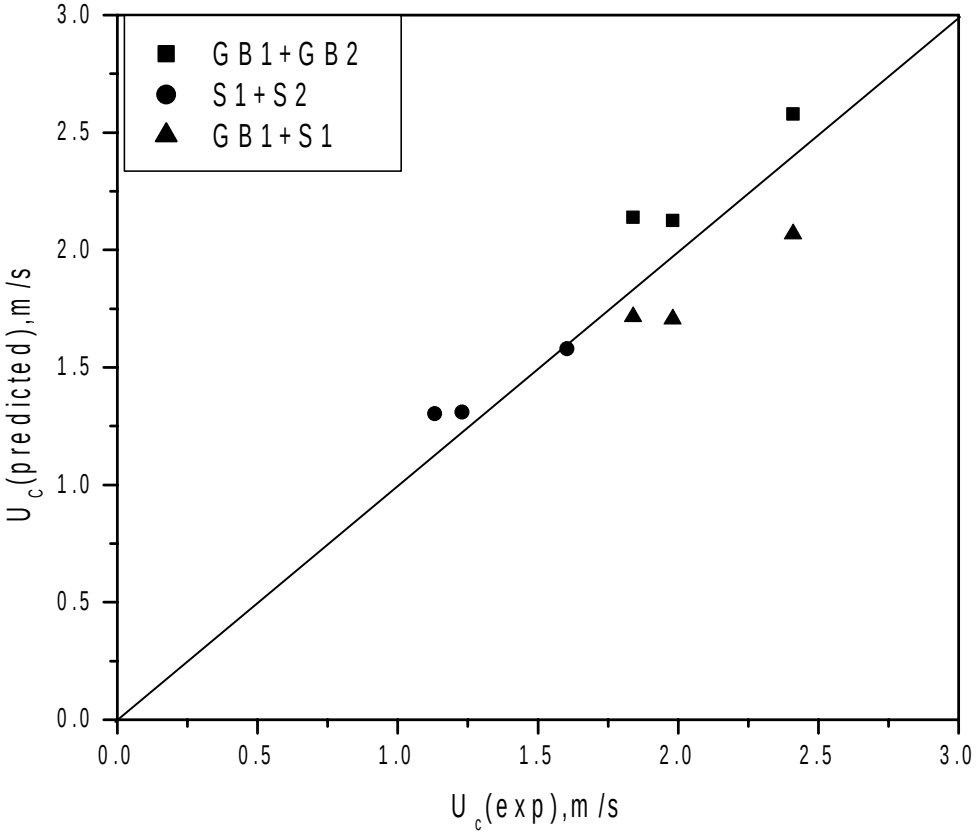
GB1+GB2
S1+S2
GB1+S1
3.0
2.5
2.0
1.5
1.0
0.5
0.0
0.0
0.5
1.0
1.5
2.0
2.5
3.0
U_c(predicted),m/s
U_c(exp),m/s

Figure-9.

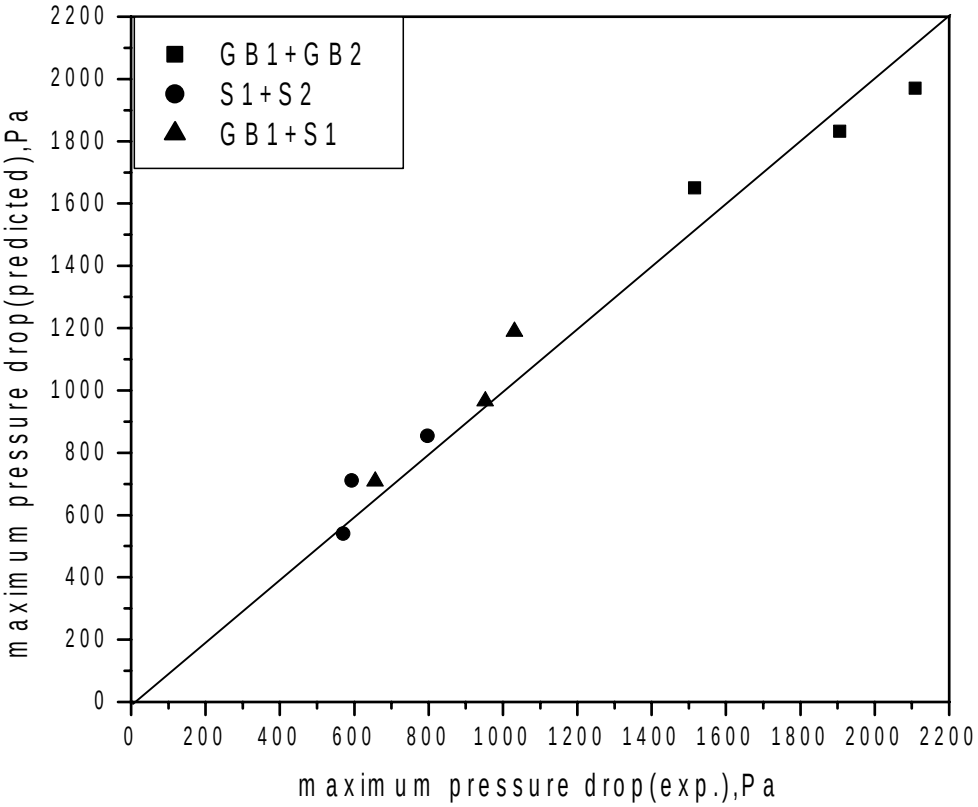
GB1+GB2
S1+S2
GB1+S1
maximum pressure drop(predicted),Pa
maximum pressure drop(exp.),Pa
0
200
400
600
800
1000
1200
1400
1600
1800
2000
2200

Figure 10.

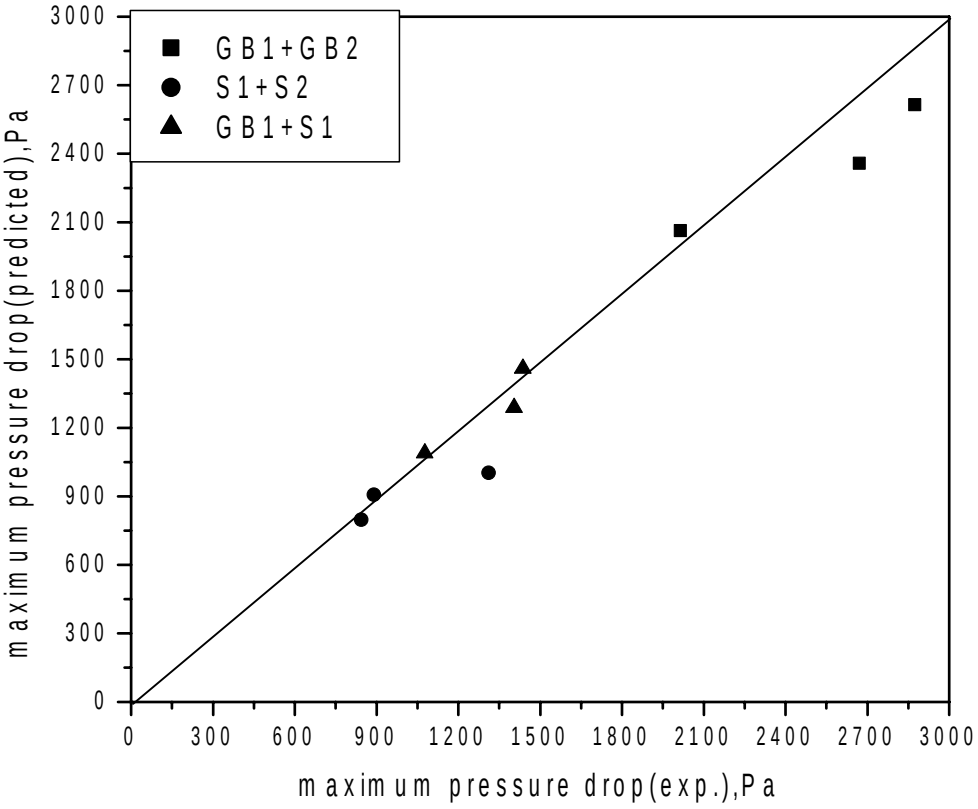
GB1+GB2
S1+S2
GB1+S1
maximum pressure drop(predicted),Pa
maximum pressure drop(exp.),Pa
0
300
600
900
1200
1500
1800
2100
2400
2700
3000

Figure 11.

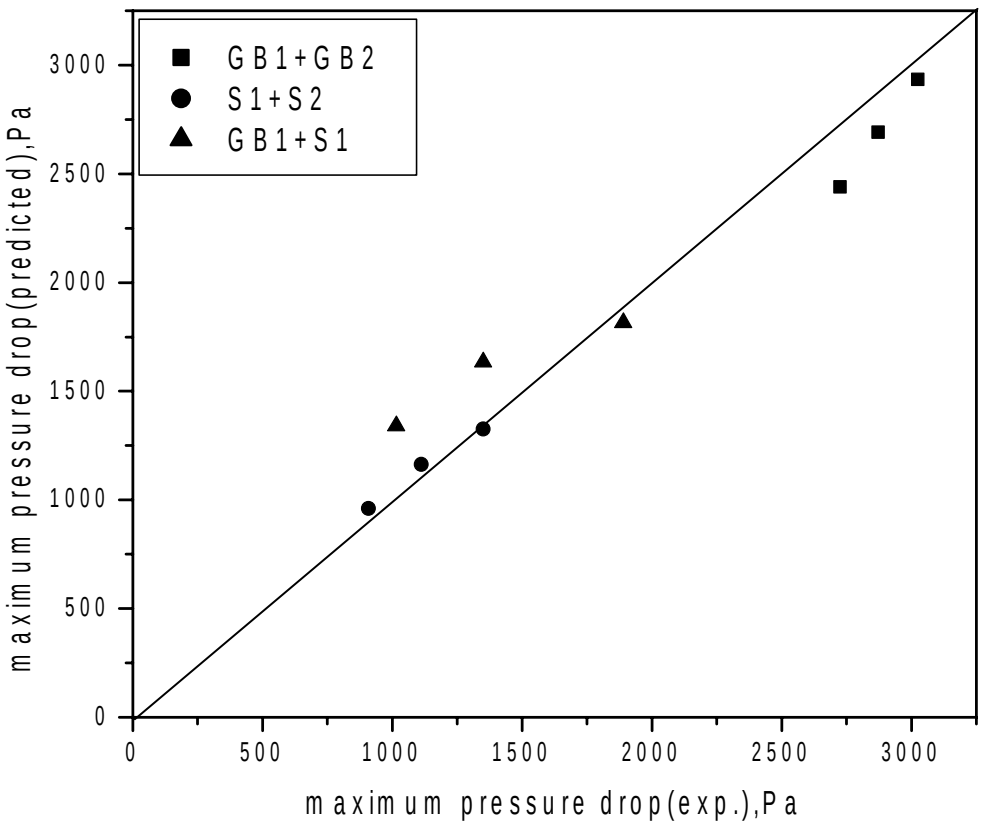
GB1+GB2
S1+S2
GB1+S1
maximum pressure drop(predicted),Pa
maximum pressure drop(exp.),Pa
0
500
1000
1500
2000
2500
3000

Figure 12.

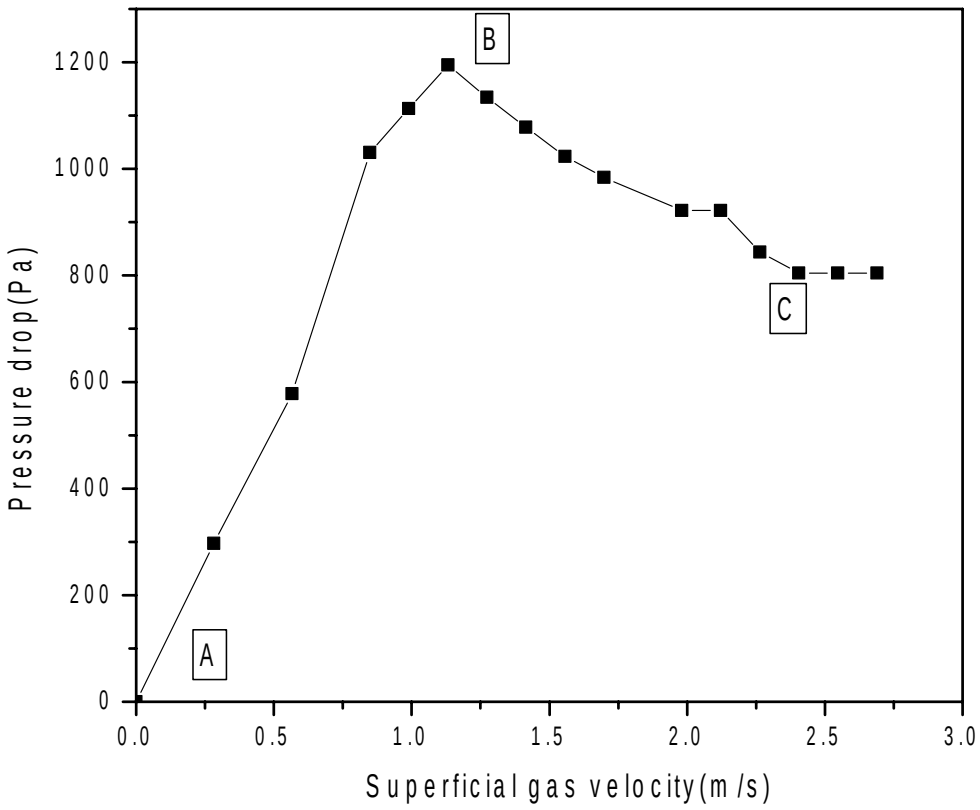
B
A
C
1200
1000
800
600
400
200
0
0.0
0.5
1.0
1.5
2.0
2.5
3.0
Pressure drop(Pa)
Superficial gas velocity(m/s)

Figure-13.

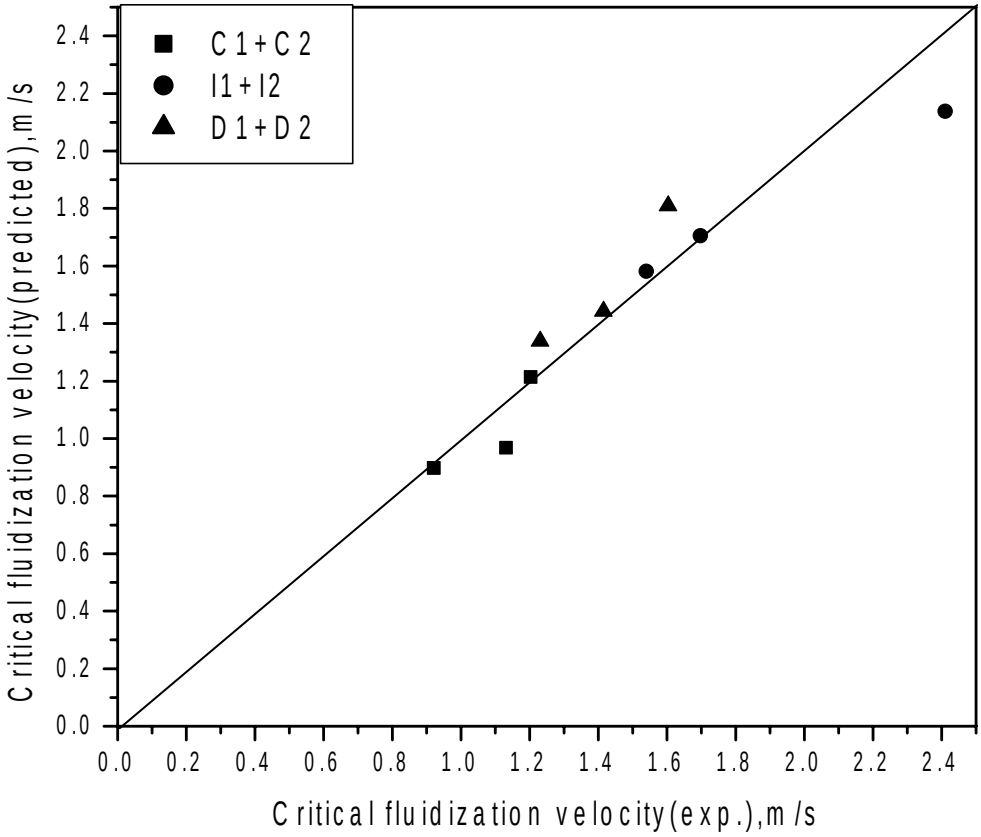
C 1 + C 2
I 1 + I 2
D 1 + D 2
Critical fluidization velocity(predicted),m/s
Critical fluidization velocity(exp.),m/s
0.0
0.2
0.4
0.6
0.8
1.0
1.2
1.4
1.6
1.8
2.0
2.2
2.4

Figure-14.

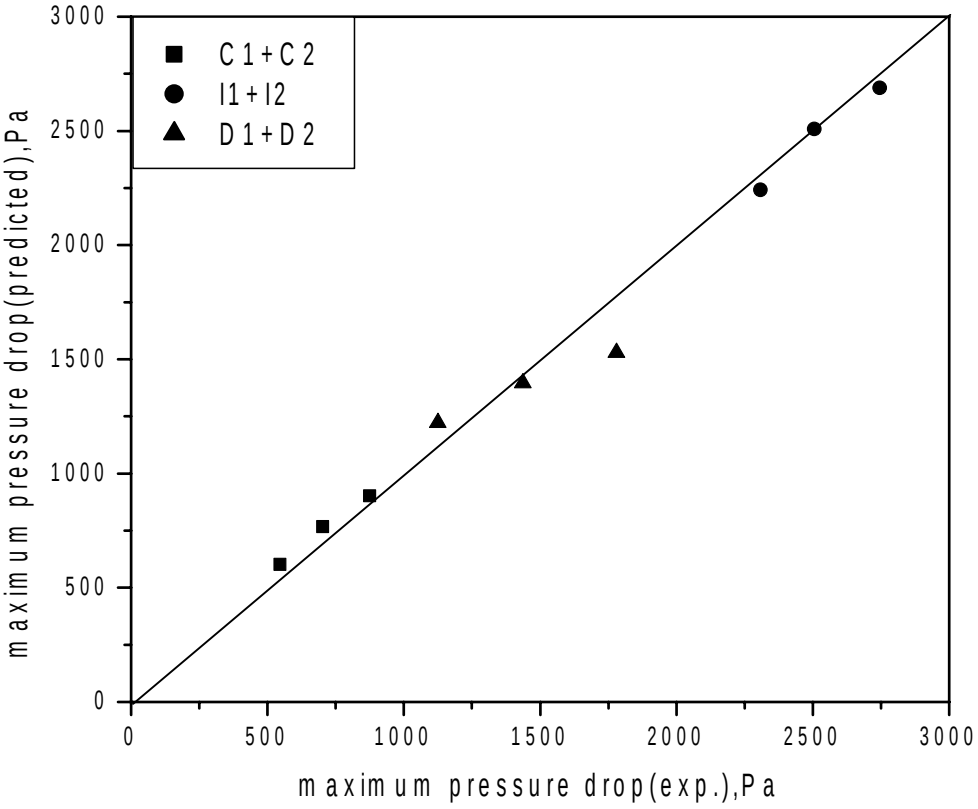
C1+C2
I1+I2
D1+D2
maximum pressure drop(predicted),Pa
maximum pressure drop(exp.),Pa
0
500
1000
1500
2000
2500
3000

Figure-15

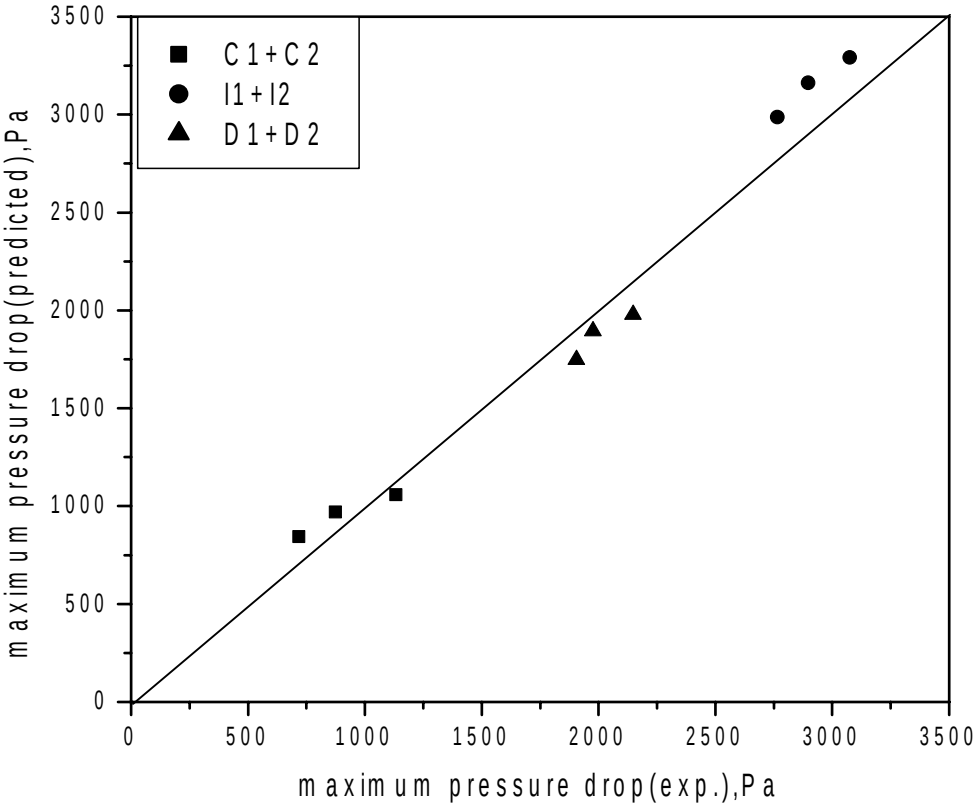
C 1 + C 2
I1 + I2
D 1 + D 2
maximum pressure drop(predicted),Pa
maximum pressure drop(exp.),Pa
0
500
1000
1500
2000
2500
3000
3500

Figure-16

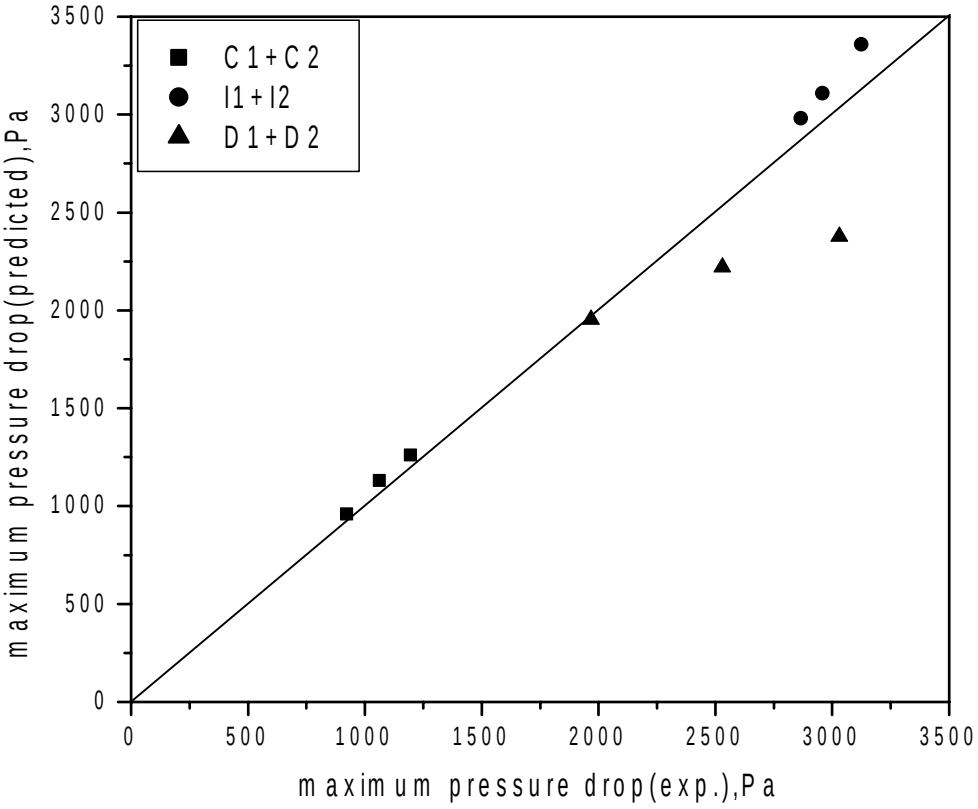
C1+C2
I1+I2
D1+D2
maximum pressure drop(predicted),Pa
maximum pressure drop(exp.),Pa
0
500
1000
1500
2000
2500
3000
3500

Figure-17

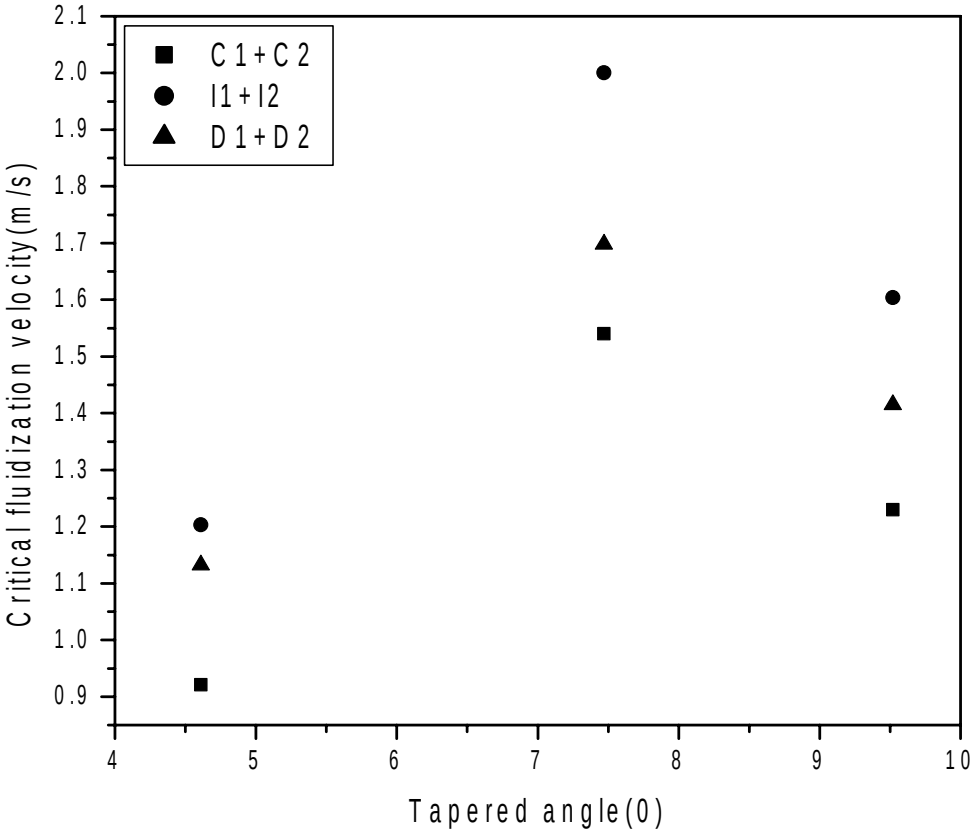
C 1 + C 2
I1 + I2
D 1 + D 2
Critical fluidization velocity(m/s)
Tapered angle(0)
2.1
2.0
1.9
1.8
1.7
1.6
1.5
1.4
1.3
1.2
1.1
1.0
0.9
4
5
6
7
8
9
10

Fig-18

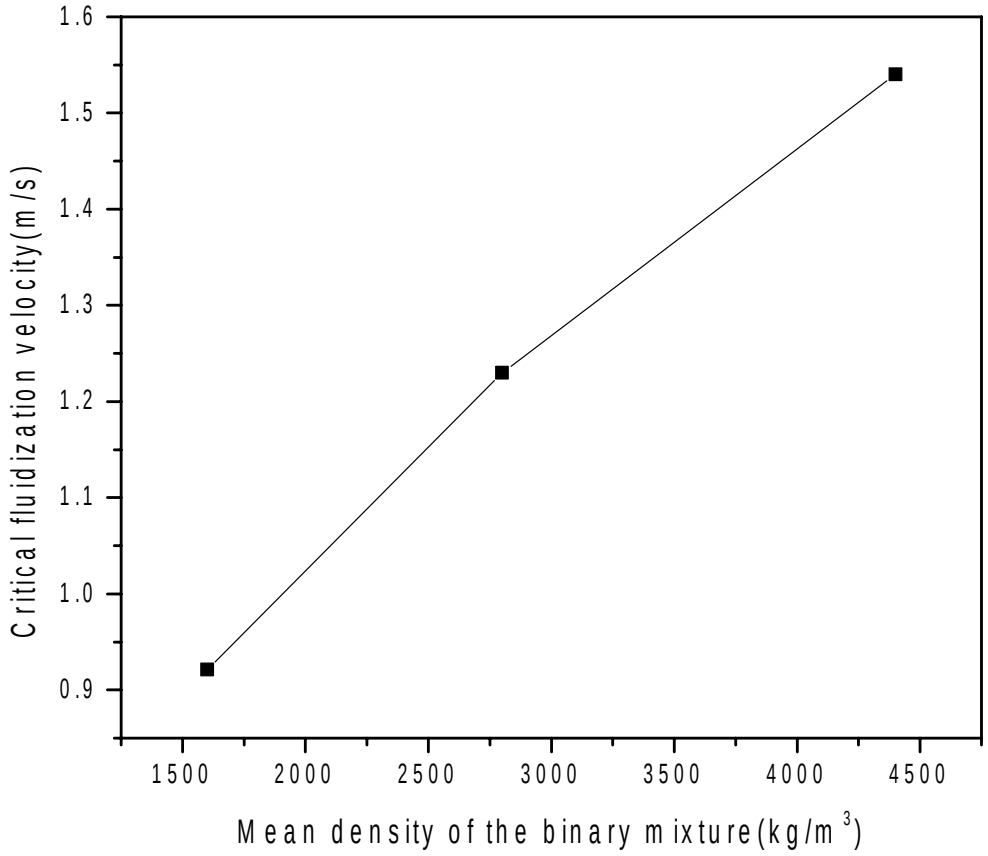
1.6
1.5
1.4
1.3
1.2
1.1
1.0
0.9
Critical fluidization velocity(m/s)
1500
2000
2500
3000
3500
4000
4500
Mean density of the binary mixture(kg/m 3)

Figure 19

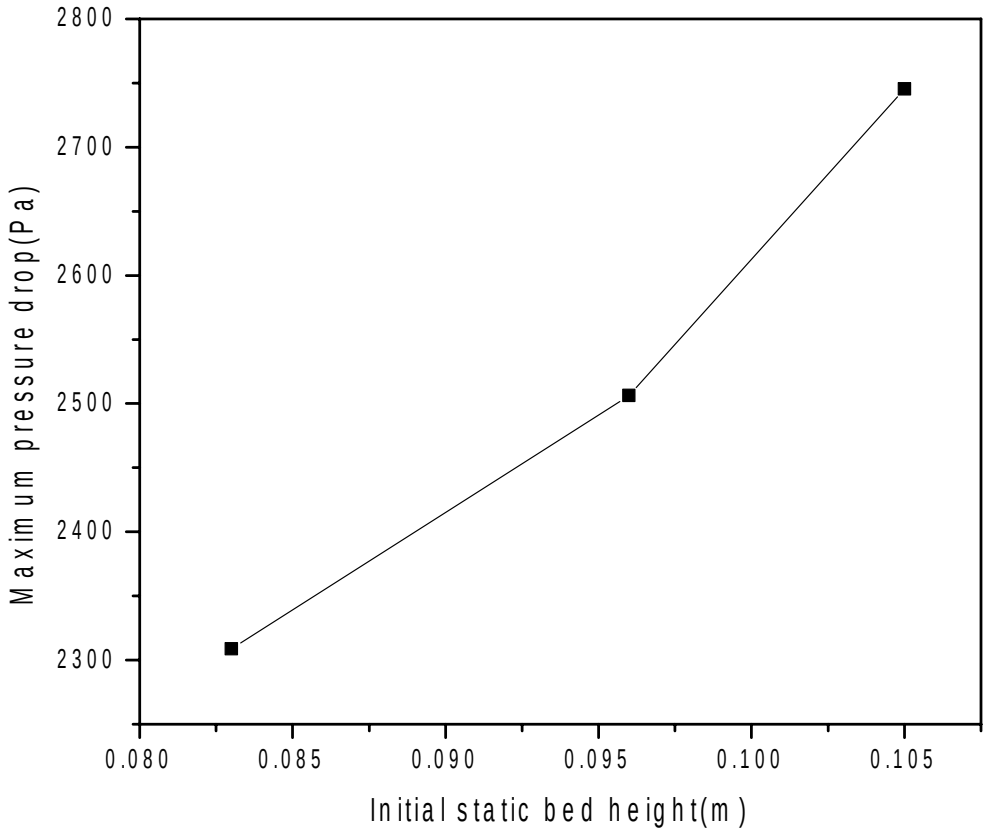
2800
2700
2600
2500
2400
2300
Maximum pressure drop(Pa)
0.080
0.085
0.090
0.095
0.100
0.105
Initial static bed height(m)

Figure -20

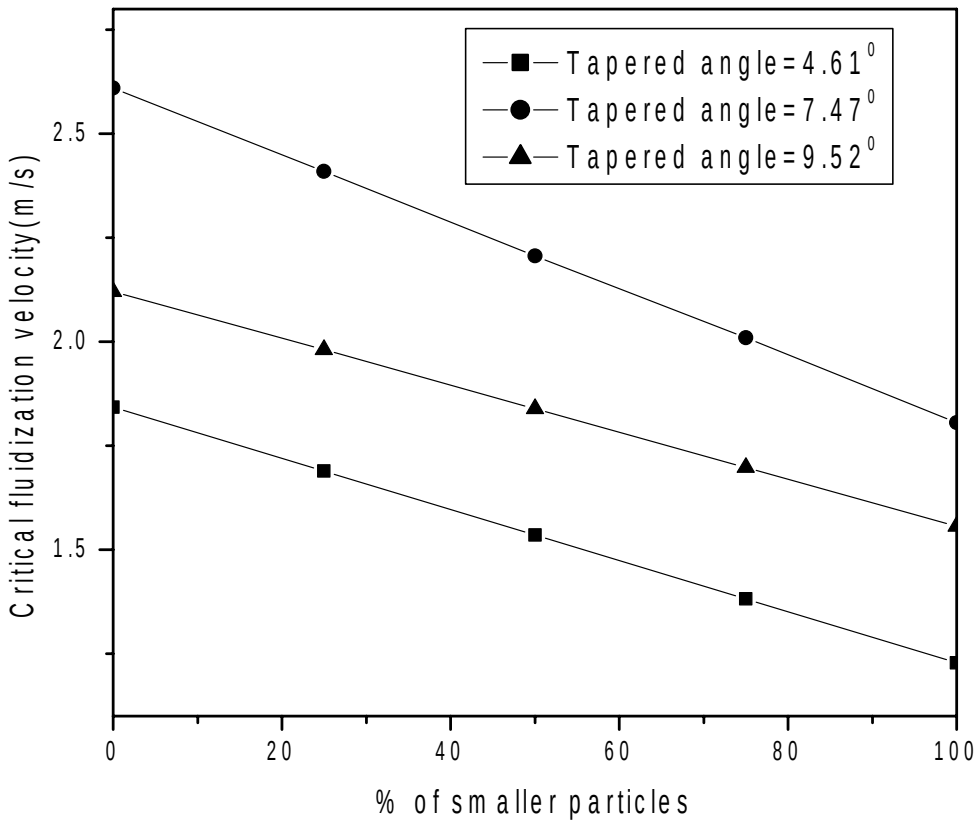
Tapered angle=4.61°
Tapered angle=7.47°
Tapered angle=9.52°
Critical fluidization velocity(m/s)
2.5
2.0
1.5
0
20
40
60
80
100
% of smaller particles

Figure -21

Table 1A

Dimensions of the tapered column

| Dimension | Tapered angle (Θ) | | |
|---|---|---|---|
| | 4.61 | 7.47 | 9.52 |
| Bottom diameter,mm | 48 | 42 | 50 |
| Top diameter,mm | 132 | 174 | 212 |
| Reactor height,mm | 520 | 504 | 483 |

Table 1B

Properties of the particles

| Material | Diameter, $\mu$m | Density,kg/m$^3$ | Range of Minimum fluidization velocity ,Umf(m/s) | Terminal velocity(m/s) |
|---|---|---|---|---|
| Coal | 1718 | 1600 | 0.849-2.01 | 8.39 |
| Coal | 1303 | 1600 | 0.566-1.228 | 7.31 |
| Iron ore | 1718 | 4400 | 1.415-2.407 | 13.92 |
| Iron ore | 1303 | 4400 | 1.228-2.01 | 12.13 |
| Dolomite | 1718 | 2800 | 1.228-2.407 | 11.11 |
| Dolomite | 1303 | 2800 | 1.132-2.01 | 9.67 |

Table 2

Comparison of critical fluidization velocity with experimental results in absolute error (%)

| Materials | Composition (weight %) | Hs(m) | $\alpha$ (deg) | Uc(exp.),m/s | Uc(predicted value),m/s | absolute error (%) |
|---|---|---|---|---|---|---|
| GB1+GB2 | 50+50 | 0.096 | 4.61 | 1.84 | 2.139 | 16.25 |
| | | 0.11 | 4.61 | 1.84 | 2.139 | 16.25 |
| | | 0.121 | 4.61 | 1.84 | 2.139 | 16.25 |
| S1+S2 | | 0.072 | 4.61 | 1.23 | 1.31 | 6.50 |
| | | 0.103 | 4.61 | 1.23 | 1.31 | 6.50 |
| | | 0.131 | 4.61 | 1.23 | 1.31 | 6.50 |
| GB1+GB2 | 50+50 | 0.105 | 7.47 | 2.41 | 2.578 | 6.97 |
| | | 0.125 | 7.47 | 2.41 | 2.578 | 6.97 |
| | | 0.143 | 7.47 | 2.41 | 2.578 | 6.97 |
| S1+S2 | 50+50 | 0.098 | 7.47 | 1.604 | 1.579 | 1.56 |
| | | 0.116 | 7.47 | 1.604 | 1.579 | 1.56 |
| | | 0.132 | 7.47 | 1.604 | 1.579 | 1.56 |
| GB1+GB2 | 50+50 | 0.11 | 9.52 | 1.981 | 2.126 | 7.32 |
| | | 0.125 | 9.52 | 1.981 | 2.126 | 7.32 |
| | | 0.14 | 9.52 | 1.981 | 2.126 | 7.32 |
| S1+S2 | 50+50 | 0.105 | 9.52 | 1.132 | 1.302 | 15.02 |
| | | 0.135 | 9.52 | 1.132 | 1.302 | 15.02 |
| | | 0.16 | 9.52 | 1.132 | 1.302 | 15.02 |
| GB1+S1 | 50+50 | 0.06 | 4.61 | 1.84 | 1.716 | 6.74 |
| | | 0.09 | 4.61 | 1.84 | 1.716 | 6.74 |
| | | 0.118 | 4.61 | 1.84 | 1.716 | 6.74 |
| | 50+50 | 0.086 | 7.47 | 2.41 | 2.068 | 14.19 |
| | | 0.107 | 7.47 | 2.41 | 2.068 | 14.19 |
| | | 0.126 | 7.47 | 2.41 | 2.068 | 14.19 |
| | 50+50 | 0.095 | 9.52 | 1.981 | 1.705 | 13.93 |
| | | 0.123 | 9.52 | 1.981 | 1.705 | 13.93 |
| | | 0.141 | 9.52 | 1.981 | 1.705 | 13.93 |

Table 3

Comparison of maximum pressure drop with experimental results in absolute error (%)

| Materials | Composition (weight %) | Hs(m) | $\alpha$ (deg) | $\Delta$ Pmax (exp.),Pa | $\Delta$ Pmax (predicted value),Pa | absolute error (%) |
|---|---|---|---|---|---|---|
| GB1+GB2 | 50+50 | 0.096 | 4.61 | 1515.26 | 1650.42 | 8.92 |
| | | 0.11 | 4.61 | 1905.79 | 1831.89 | 3.88 |
| | | 0.121 | 4.61 | 2108.86 | 1970.69 | 6.55 |
| S1+S2 | 50+50 | 0.072 | 4.61 | 570.18 | 539.80 | 5.33 |
| | | 0.103 | 4.61 | 593.6 | 710.23 | 19.65 |
| | | 0.131 | 4.61 | 796.68 | 853.94 | 7.19 |
| GB1+GB2 | 50+50 | 0.105 | 7.47 | 2015.14 | 2063.18 | 2.38 |
| | | 0.125 | 7.47 | 2671.23 | 2358.10 | 11.72 |
| | | 0.143 | 7.47 | 2874.44 | 2614.17 | 9.05 |
| S1+S2 | 50+50 | 0.098 | 7.47 | 843.54 | 797.92 | 5.41 |
| | | 0.116 | 7.47 | 890.41 | 907.49 | 1.92 |
| | | 0.132 | 7.47 | 1312.18 | 1002.49 | 23.60 |
| GB1+GB2 | 50+50 | 0.11 | 9.52 | 2725.24 | 2439.66 | 10.48 |
| | | 0.125 | 9.52 | 2872.44 | 2690.75 | 6.33 |
| | | 0.14 | 9.52 | 3025.32 | 2934.87 | 2.99 |
| S1+S2 | 50+50 | 0.105 | 9.52 | 908.73 | 959.91 | 5.63 |
| | | 0.135 | 9.52 | 1112.35 | 1163.77 | 4.62 |
| | | 0.16 | 9.52 | 1350.87 | 1325.59 | 1.87 |
| GB1+S1 | 50+50 | 0.06 | 4.61 | 656.09 | 707.86 | 7.89 |
| | | 0.09 | 4.61 | 952.89 | 965.79 | 1.35 |
| | | 0.118 | 4.61 | 1030.99 | 1189.59 | 15.38 |
| | | 0.086 | 7.47 | 1077.86 | 1088.62 | 0.99 |
| | | 0.107 | 7.47 | 1405.15 | 1287.02 | 8.41 |
| | | 0.126 | 7.47 | 1437.15 | 1458.76 | 1.50 |
| | | 0.095 | 9.52 | 1015.38 | 1340.63 | 32.03 |
| | | 0.123 | 9.52 | 1351.23 | 1634.08 | 20.93 |
| | | 0.141 | 9.52 | 1890.17 | 1814.37 | 4.01 |

Table 4

Comparison of critical fluidization velocity with experimental results in absolute error (%)

| materials | composition (weight %) | Hs(m) | $\alpha$ (deg) | Uc(exp) | Uc(predicted value) | absolute error (%) |
|---|---|---|---|---|---|---|
| C1+C2 | 50+50 | 0.095 | 4.61 | 0.921 | 0.897 | 2.61 |
| | | 0.13 | 4.61 | 0.921 | 0.897 | 2.61 |
| | | 0.16 | 4.61 | 0.921 | 0.897 | 2.61 |
| I1+I2 | 50+50 | 0.083 | 4.61 | 1.54 | 1.581 | 2.66 |
| | | 0.096 | 4.61 | 1.54 | 1.581 | 2.66 |
| | | 0.105 | 4.61 | 1.54 | 1.581 | 2.66 |
| D1+D2 | 50+50 | 0.08 | 4.61 | 1.23 | 1.338 | 8.78 |
| | | 0.095 | 4.61 | 1.23 | 1.338 | 8.78 |
| | | 0.107 | 4.61 | 1.23 | 1.338 | 8.78 |
| C1+C2 | 50+50 | 0.127 | 7.47 | 1.203 | 1.213 | 0.83 |
| | | 0.152 | 7.47 | 1.203 | 1.213 | 0.83 |
| | | 0.17 | 7.47 | 1.203 | 1.213 | 0.83 |
| I1+I2 | 50+50 | 0.104 | 7.47 | 2.41 | 2.138 | 11.29 |
| | | 0.112 | 7.47 | 2.41 | 2.138 | 11.29 |
| | | 0.118 | 7.47 | 2.41 | 2.138 | 11.29 |
| D1+D2 | 50+50 | 0.11 | 7.47 | 1.604 | 1.809 | 12.78 |
| | | 0.122 | 7.47 | 1.604 | 1.809 | 12.78 |
| | | 0.129 | 7.47 | 1.604 | 1.809 | 12.78 |
| C1+C2 | 50+50 | 0.13 | 9.52 | 1.132 | 0.967 | 14.58 |
| | | 0.161 | 9.52 | 1.132 | 0.967 | 14.58 |
| | | 0.185 | 9.52 | 1.132 | 0.967 | 14.58 |
| I1+I2 | 50+50 | 0.090 | 9.52 | 1.698 | 1.705 | 0.41 |
| | | 0.095 | 9.52 | 1.698 | 1.705 | 0.41 |
| | | 0.105 | 9.52 | 1.698 | 1.705 | 0.41 |
| D1+D2 | 50+50 | 0.11 | 9.52 | 1.415 | 1.443 | 1.98 |
| | | 0.13 | 9.52 | 1.415 | 1.443 | 1.98 |
| | | 0.142 | 9.52 | 1.415 | 1.443 | 1.98 |

Table 5

Comparison of maximum pressure drop with experimental results in absolute error (%)

| materials | Composition (weight %) | Hs(m) | $\alpha$ (deg) | $\Delta$ Pmax (exp) | $\Delta$ Pmax (predicted value) | absolute error (%) |
|---|---|---|---|---|---|---|
| C1+C2 | 50+50 | 0.095 | 4.61 | 546.74 | 602.43 | 10.18 |
| | | 0.13 | 4.61 | 702.95 | 767.65 | 9.2 |
| | | 0.16 | 4.61 | 874.79 | 901.24 | 3.02 |
| I1+I2 | 50+50 | 0.083 | 4.61 | 2308.58 | 2241.02 | 2.93 |
| | | 0.096 | 4.61 | 2506.32 | 2507.69 | 0.05 |
| | | 0.105 | 4.61 | 2745.25 | 2687.49 | 2.10 |
| D1+D2 | 50+50 | 0.08 | 4.61 | 1124.73 | 1221.45 | 8.59 |
| | | 0.095 | 4.61 | 1437.15 | 1394.91 | 2.94 |
| | | 0.107 | 4.61 | 1780.82 | 1529.19 | 14.13 |
| C1+C2 | 50+50 | 0.127 | 7.47 | 718.58 | 843.89 | 17.44 |
| | | 0.152 | 7.47 | 874.79 | 969.58 | 10.84 |
| | | 0.17 | 7.47 | 1132.54 | 1057.16 | 6.65 |
| I1+I2 | 50+50 | 0.104 | 7.47 | 2765.54 | 2986.02 | 7.97 |
| | | 0.112 | 7.47 | 2896.51 | 3161.99 | 9.17 |
| | | 0.118 | 7.47 | 3075.42 | 3292.11 | 7.05 |
| D1+D2 | 50+50 | 0.11 | 7.47 | 1905.79 | 1748.64 | 8.25 |
| | | 0.122 | 7.47 | 1976.08 | 1894.29 | 4.14 |
| | | 0.129 | 7.47 | 2147.92 | 1977.73 | 7.92 |
| C1+C2 | 50+50 | 0.13 | 9.52 | 921.65 | 959.05 | 4.06 |
| | | 0.161 | 9.52 | 1062.24 | 1131.39 | 6.51 |
| | | 0.185 | 9.52 | 1195.02 | 1259.63 | 5.41 |
| I1+I2 | 50+50 | 0.090 | 9.52 | 2865.12 | 2980.57 | 4.03 |
| | | 0.095 | 9.52 | 2958.54 | 3107.73 | 5.04 |
| | | 0.105 | 9.52 | 3125.28 | 3357.59 | 7.43 |
| D1+D2 | 50+50 | 0.11 | 9.52 | 1968.27 | 1951.75 | 0.84 |
| | | 0.13 | 9.52 | 2530.63 | 2220.67 | 12.25 |
| | | 0.142 | 9.52 | 3030.51 | 2377.46 | 21.55 |

# REFERENCES


[1] Y.Peng, L.T.Fan, Hydrodynamic characteristics of fluidization in liquid-solid tapered beds, Chemical Engineering Science 52 (14) (1997) 2277 – 2290.

[2] M. Olazar, M.J. San Jose, A.T.J. Aguayo, M. Arandes, J.Bilbao, Ind. Eng. Chem. Res. 31 (1992) 1784–1792.

[3]M.Olazer, M.J.San Jose, A.T.Aguayo, J.M.Arandes, J.Bilbao, Pressure drop in conical spouted beds, The Chemical Engineering Journal 51 (1993) 53 – 60.

[4] N.I. Gelperin, E.N. Einstein, E.N. Gelperin, S.D. Lvova, Khim.I Tekin. Topl. I Masel. 5 (8) (1960) 51.

[5] Y. Nishi, Kagaku kogaku Ronbunshu 5 (1979) 202–204.

[6] M. Kwauk, Fluidization 1993 91–100, Science and Press, NewYork.

[7] Y.F. Shi, Y.S. Yu, L.T. Fan, Incipient fluidization condition for a tapered fluidized bed, Ind. Eng. Chem. Fundam. 23 (1984) 484–489.

[8] K.C. Biswal, T. Bhowmik, G.K. Roy, Prediction of minimum fluidization velocity for gas–solid fluidization of regular particles in conical vessels, Chem. Eng. J. 30 (1985) 57–62.

[9] K.C. Biswal, T. Bhowmik, G.K. Roy, Prediction of pressure drop for a conical fixed bed of spherical particles in gas–solid systems, Chem. Eng. J. 29 (1984) 47–50.

[10] A.E. Gorshtein, I.P. Mukhlenov, Hydraulic resistance of a fluidized bed in a cyclone without a grate. II. Critical gas rate corresponding to the beginning of a jet formation, Zh. Prikl. Khim. (Leningrad) 37 (1964) 1887–1893.

[11] S. Jing, Q. Hu, J.Wang, Y. Jin, Fluidization of coarse particles in gas–solid conical beds, Chem. Eng. Process. 39 (2000) 379–387.

12] J. Shan, C. Guobin, M.Fan, B.Yu, W. Jingfu, J. Yong, Fluidization of fine particles in conical beds, Powder Technology 118 (2001) 271 – 274.

[13]F.Depypere, J.G.Pieters, K.Dewettinck, Expanded bed height determination in a tapered fluidized bed reactor, Journal of Food Engineering 67 (2005) 353 – 359.

[14] H.G.Kim, I.O.Lee, U.C.Chung and Y.H.Kim, Fluidization characteristics of iron ore fines of wide size distribution in a cold tapered gas-solid fluidized bed, ISIJ International 40(2000)16-22.

[15] S.Chiba,T.Chiba,A.W.Nienow and H.Kobayashi, The critical fluidization velocity, bed expansion and pressure-drop profiles of binary particle mixtures, Powder Technology,22(1979)255-269.

[16] K.Noda, S.Uchida, T.Makino and H.Kamo, Critical fluidization velocity of binary particles with large size ratio, Powder Technology, 46(1986) 149-154.

[17] D.Bai, Y.Masuda, N.Nakagawa and K.Kato, Hydrodynamic behavior of a binary solids fluidized bed, Journal of Chemical Engineering of Japan, 29(1996) 211-216.

[18] V.Thonglimp, N.Hiquily and C.Laguerie, Vitesse minimale de fluidization et expansion des couches de mélanges de particules solids fluidisees par un gaz, Powder Technology 39(1984) 223-239.

[19] J.Rincon, J.Guardiola, A.Romero and G.Ramos, Predicting the critical fluidization velocity of multicomponent systems, Journal of Chemical Engineering of Japan, 27(1994)177-181.

[20] R.Deiva Venkatesh, J.Chaouki, D.Klvana, Fluidization of cryogel in a conical column, Powder technology 89(1996) 179-186.

[21] M.Olazer,R.Aguado,M.J.San Jose,S.Alvarez,J.Bilbao, Critical spouting velocity for the pyrolysis of scrap tyres with sand in conical beds, Powder Technology,165(2006) 128-132.

[22] J.Li, B.Yang, G.Cheng, Affinity adsorption and hydrodynamic behavior in a tapered-bed of upward flow, Biochemical Engineering Journal 15(2003) 185-192.

[23] W.R.A.Goossens, G.L.Dumont, G.L., Spaepen, Fluidization of binary mixtures in the laminar flow region, Chem.Eng.Prog.Symp.Ser. 67(1971) 38-45.

[24] D.S.Povrenovic, D.E.Hadzismajlovic, Z.B.Grbavcic, D.V.Vukovic, Critical fluid flow rate, pressure drop and stability of a conical spouted Bed, The Canadian Journal of Chemical Engineering 70 (1992) 216 – 222.

[25] G.R.Caicedo, M.G.Ruiz, J.J.P.Marques, J.G.Soler, Critical fluidization velocities for gas-solid 2D beds, Chemical Engineering and Processing 41 (2002) 761 – 764.

[26] Babu, S. P., Leipsiger, S., Lee, B. S., Weil, S. A. (1973), 'Solids mixing in batch operated tapered bed and non- tapered gas fluidized beds'. *Fluidized Bed Fundam. Appl*. AIChE Symp.Ser.69, 49-57.

[27] Biswal K.C., Sahu, S., Roy, G. K. (1982), 'Prediction of fluctuation ratio for gas solid fluidization of regular particles in conical vessels', *The Chemical Engineering Journal*, 23, 97-100.

[28] Biswal.K.C, Samal, B. B., Roy, G. K. (1984), 'Dynamics of gas-solid fluidization of regular particles in conical vessels', *The Journal the IE (India),* Vol. 65, CH-1, 15 -17.

[29] Biswal K.C. and Roy, G. K. (1985), 'Prediction of fluctuation ratio for gas-solid fluidizations of irregular particles in conical vessels'. *The Journal of the IE (India)*, Vol. 65, CH-2, 57-62.

[30] Hsu H. W., (1978), 'Characteristics of tapered fluidized reactors; two–phase systems'. *Biotechnology Bioengineers' Symposium*, 8, 1 – 11.

[31] Koloini T. and Farkas E. J. (1973), 'Fixed bed pressure drops a liquid fluidization in tapered or conical vessels'. *Canadian Journal of Chemical Engineering*, 51, 499-502.

[32] Maruyama T.and Koyanagi T (1993). 'Fluidization in tapered vessels'. *The Chemical Engineering Journal*.51, 121-128.

[33] C.D. Scott, C.W. Hancher, Use of a tapered fluidized bed as a continuous bioreactor, Biotechnol. Bioeng. 18 (1976) 1393–1403.

[34] K. Ridgway, The tapered fluidized bed—a new processing tool, Chem. Process. Eng. 6 (1965) 317–321.

[35] S.P. Babu, S. Leipsiger, B.S. Lee, S.A.Weil, Solids mixing in batch operated tapered bed and non-tapered gas fluidized beds, Fluidized Bed Fundam.Appl. AIChE, Symp. Ser. 69 (1973) 49–57.

[36] T. Maruyama, H. Sato, Liquid fluidization in conical vessels, Chem. Eng.J. 46 (1991) 15–21.

[37] T. Koloini, E.J. Farkas, Fixed bed pressure drop of a liquid fluidization in tapered or conical vessels, Can. J. Chem. Eng. 51 (1973) 499–502.

[38] Y.F. Shi, Y.S. Yu, L.T. Fan, Incipient fluidization condition for a tapered fluidized bed, Ind. Eng. Chem. Fundam. 23 (1984) 484–489.

[39] K.C. Biswal, T. Bhowmik, G.K. Roy, Prediction of minimum fluidization velocity for gas–solid fluidization of regular particles in conical vessels, Chem. Eng. J. 30 (1985) 57–62.

[40] K.C. Biswal, T. Bhowmik, G.K. Roy, Prediction of pressure drop for a conical fixed bed of spherical particles in gas–solid systems, Chem. Eng.
J. 29 (1984) 47–50.

[41] R.K. Singh, A. Suryanarayana, G.K. Roy, Prediction of minimum velocity and minimum bed pressure drop for gas–solid fluidization in conical conduits, Can. J. Chem. Eng. 70 (1992) 185–189.

[42] J. Shan, C. Guobin, M. Fan, B. Yu,W. Jingfu, J. Yong, Fluidization of fine
particles in conical beds, Powder Technol. 118 (2001) 271–274.

[43] G. Narsimhan, On generalized expression for prediction of minimum fluidization velocity, AIChE J. 11 (1965) 550–554.
[44] J. Li, B. Yang, G. Cheng, Affinity adsorption and hydrodynamic behavior in a tapered-bed of upward flow, Biochem. Eng. J. 15 (2003) 185–192.
[45] D.S. Povrenovic, D.E. Hadzismajlovic, Z.B. Grbavcic, D.V. Vukovic, Minimum fluid flow rate, pressure drop and stability of a conical spouted bed, Can. J. Chem. Eng. 70 (1992) 216–222.
[46] G.R. Caicedo, M.G. Ruiz, J.J.P. Marqu´es, J.G. Soler, Minimum fluidization velocities for gas–solid 2D beds, Chem. Eng. Process. 41 (2002) 761–764.
[47] Fluent Inc.,"Fluent 6.1 UDF Manual"(2003a)
[48] Fluent Inc.,"Fluent 6.1 user guide"(2003b)